Chapter 9 Radar Clutter

Clutter is a term used to describe any object that may generate unwanted radar returns that may interfere with normal radar operations. Parasitic returns that enter the radar through the antenna's mainlobe are called main-lobe clutter; otherwise they are called sidelobe clutter. Clutter can be classified into two main categories: surface clutter and airborne or volume clutter. Surface clutter includes trees, vegetation, ground terrain, man-made structures, and sea surface (sea clutter). Volume clutter normally has a large extent (size) and includes chaff, rain, birds, and insects. Surface clutter changes from one area to another, while volume clutter may be more predictable.

Clutter echoes are random and have thermal noise-like characteristics because the individual clutter components (scatterers) have random phases and amplitudes. In many cases, the clutter signal level is much higher than the receiver noise level. Thus, the radar's ability to detect targets embedded in high clutter background depends on the Signal-to-Clutter Ratio (SCR) rather than the SNR.

9.1. Clutter Cross Section Density

Since clutter returns are target-like echoes, the only way a radar can distinguish target returns from clutter echoes is based on the target RCS σ_t and the anticipated clutter RCS σ_c. Clutter RCS can be defined as the equivalent radar cross section attributed to reflections from a clutter area, A_c. The average clutter RCS is given by

$$\sigma_c = \sigma^0 A_c \tag{9.1}$$

where σ^0 is the clutter scattering coefficient, a dimensionless quantity that is often expressed in dB. The equivalent of Eq. (9.1) for volume clutter is

$$\sigma_c = \eta^0 V_w \tag{9.2}$$

where V_w is the clutter volume and η^0 is the volume clutter scattering coefficient. Note that η^0 units are m^{-1}, and because of this, it is typically expressed in dB/meter units.

9.2. Surface Clutter

Surface clutter includes both land and sea clutter, and is often called area clutter. Area clutter manifests itself in airborne radars in the look-down mode. It is also a major concern for ground-based radars when searching for targets at low grazing angles. The grazing angle ψ_g is the angle from the surface of the earth to the main axis of the illuminating beam, as illustrated in Fig. 9.1.

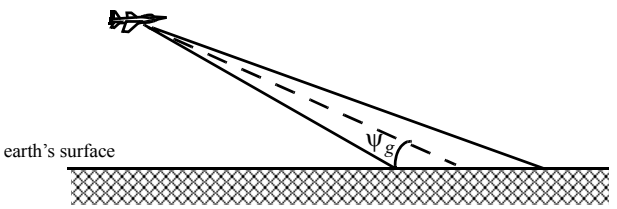

Figure 9.1. Definition of a grazing angle.

Factors that affect the radar performance due to the presence of clutter include clutter reflectivity which is function of radar wavelength, polarization, and of course shape and size of the clutter itself. The amount of clutter RCS in the radar beam depends heavily on the grazing angle, surface roughness, and spatial characteristics of clutter and its time fluctuation characteristics. Typically, the clutter scattering coefficient σ^0 is larger for smaller wavelengths. Figure 9.2 shows a sketch describing the dependency of σ^0 on the grazing angle. Three regions are identified; they are the low grazing angle region, the flat or plateau region, and the high grazing angle region.

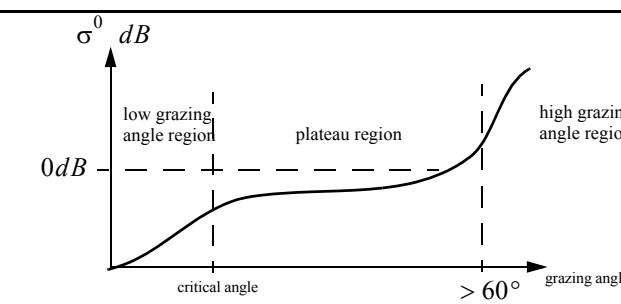

Figure 9.2. Clutter regions.

The low grazing angle region extends from zero to about the critical angle. The critical angle is defined by Rayleigh as the angle below which a surface is considered to be smooth and above which a surface is considered to be rough; Denote the root mean square (rms) of a surface height irregularity as h_{rms}; then according to the Rayleigh criteria, the surface is considered to be smooth if

$$\frac{4\pi h_{rms}}{\lambda}\sin\psi_g < \frac{\pi}{2} \tag{9.3}$$

Consider a wave incident on a rough surface, as shown in Fig. 9.3. Due to surface height irregularity (surface roughness), the rough path is longer than the smooth path by a distance $2h_{rms}\sin\psi_g$. This path difference translates into a phase differential $\Delta\psi$:

$$\Delta\psi = \frac{2\pi}{\lambda}\ 2h_{rms}\sin\psi_g \tag{9.4}$$

The critical angle ψ_{gc} is then computed when $\Delta\psi = \pi$ (first null); thus,

$$\frac{4\pi h_{rms}}{\lambda}\ \sin\psi_{gc} = \pi \tag{9.5}$$

or equivalently,

$$\psi_{gc} = \operatorname{asin}\frac{\lambda}{4h_{rms}} \tag{9.6}$$

In the case of sea clutter, for example, the rms surface height irregularity is

$$h_{rms} \approx 0.025 + 0.046\ \ S_{state}^{1.72} \tag{9.7}$$

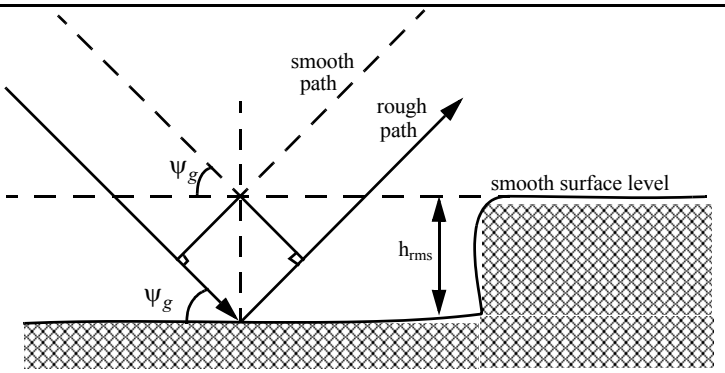

Figure 9.3. Rough surface definition.

where S_{state} is the sea state, which is tabulated in several cited references. The sea state is characterized by the wave height, period, length, particle velocity, and wind velocity. For example, $S_{state} = 3$ refers to a moderate sea state, in which the wave height is approximately $0.9144\ to\ 1.2192\ m$, the wave period 6.5 *to* 4.5 seconds, wave length $1.9812\ to\ 33.528\ m$, wave velocity $20.372\ to\ 25.928\ Km/hr$, and wind velocity $22.224\ to\ 29.632\ Km/hr$.

Clutter at low grazing angles is often referred to as diffuse clutter, where there are a large number of clutter returns in the radar beam (noncoherent reflections). In the flat region the dependency of σ^0 on the grazing angle is minimal. Clutter in the high grazing angle region is more specular (coherent reflections) and the diffuse clutter components disappear. In this region the smooth surfaces have larger σ^0 than rough surfaces, the opposite of the low grazing angle region.

9.2.1. Radar Equation for Surface Clutter

Consider an airborne radar in the look-down mode shown in Fig. 9.4. The intersection of the antenna beam with the ground defines an elliptically shaped footprint. The size of the footprint is a function of the grazing angle and the antenna $3dB$ beamwidth θ_{3dB}, as illustrated in Fig. 9.5. The footprint is divided into many ground range bins each of size $(c\tau/2)\sec\psi_g$, where τ is the pulse width. From Fig. 9.5, the clutter area A_c is

$$A_c \approx R\theta_{3dB}\frac{c\tau}{2}\sec\psi_g \tag{9.8}$$

The power received by the radar from a scatterer within A_c is given by the radar equation as

$$S_t = \frac{P_t G^2 \lambda^2 \sigma_t}{(4\pi)^3 R^4} \tag{9.9}$$

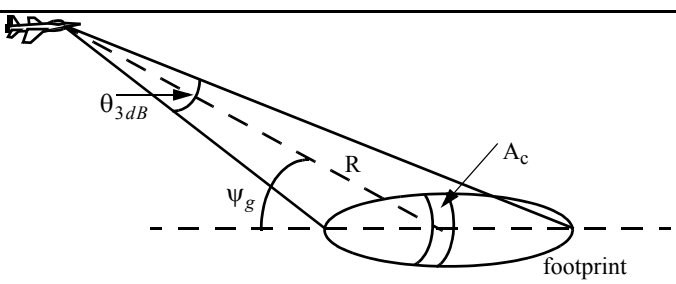

Figure 9.4. Airborne radar in the look-down mode.

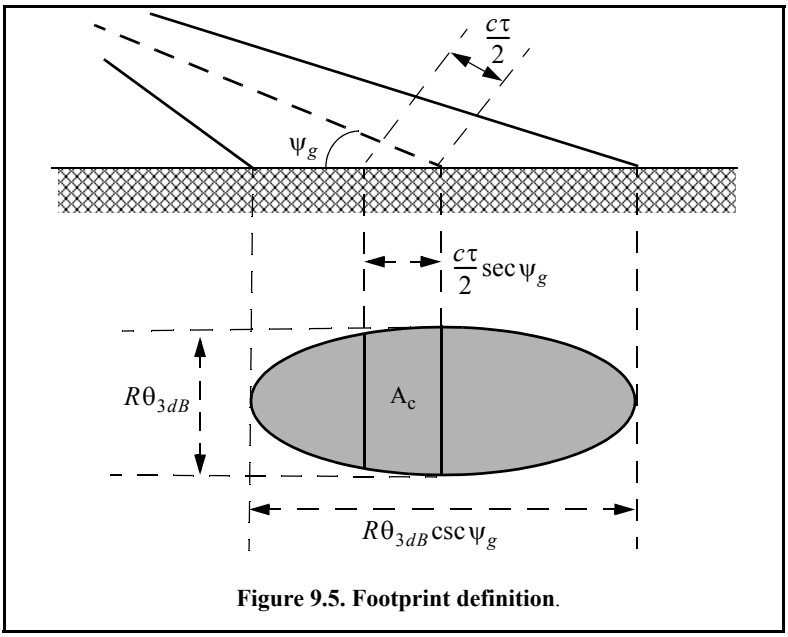

Figure 9.5. Footprint definition.

where, as usual, P_t is the peak transmitted power, G is the antenna gain, λ is the wavelength, and σ_t is the target RCS. Similarly, the received power from clutter is

$$S_C = \frac{P_t G^2 \lambda^2 \sigma_c}{(4\pi)^3 R^4} \tag{9.10}$$

where the subscript C is used for area clutter. Substituting Eq. (9.1) for σ_c into Eq. (9.10), we can then obtain the SCR for area clutter by dividing Eq. (9.9) by Eq. (9.10). More precisely,

$$(SCR)_C = \frac{2\sigma_t \cos\psi_g}{\sigma^0 \theta_{3dB} R c\tau} \tag{9.11}$$

Example:

Consider an airborne radar shown in Fig. 9.4. Let the antenna 3dB beamwidth be $\theta_{3dB} = 0.02 rad$, *the pulse width* $\tau = 2\mu s$, *range* $R = 20 Km$, *and grazing angle* $\psi_g = 20°$. *The target RCS is* $\sigma_t = 1 m^2$. *Assume that the clutter reflection coefficient is* $\sigma^0 = 0.0136$. *Compute the SCR.*

Solution:

The SCR is given by Eq. (9.11) as

$$(SCR)_C = \frac{2\sigma_t \cos\psi_g}{\sigma^0 \theta_{3dB} Rc\tau} \Rightarrow$$

$$(SCR)_C = \frac{(2)(1)(\cos 20°)}{(0.0136)(0.02)(20000)(3\times 10^8)(2\times 10^{-6})} = 5.76\times 10^{-4}$$

It follows that

$$(SCR)_C = -32.4dB$$

Thus, for reliable detection the radar must somehow increase its SCR by at least $(32+X)dB$*, where* X *is on the order of* 13 *to* $15dB$ *or better.*

9.3. Volume Clutter

Volume clutter has large extents and includes rain (weather), chaff, birds, and insects. The volume clutter coefficient is normally expressed in square meters (RCS per resolution volume). Birds, insects, and other flying particles are often referred to as angle clutter or biological clutter.

Weather or rain clutter can be suppressed by treating the rain droplets as perfect small spheres. We can use the Rayleigh approximation of a perfect sphere to estimate the rain droplets' RCS. The Rayleigh approximation, without regard to the propagation medium index of refraction is

$$\sigma = 9\pi r^2 (kr)^4 \qquad r \ll \lambda \tag{9.12}$$

where $k = 2\pi/\lambda$, and r is radius of a rain droplet.

Electromagnetic waves when reflected from a perfect sphere become strongly co-polarized (have the same polarization as the incident waves). Consequently, if the radar transmits, for example, a right-hand-circular (RHC) polarized wave, then the received waves are left-hand-circular (LHC) polarized because they are propagating in the opposite direction. Therefore, the back-scattered energy from rain droplets retains the same wave rotation (polarization) as the incident wave, but has a reversed direction of propagation. It follows that radars can suppress rain clutter by co-polarizing the radar transmit and receive antennas.

Denote η as RCS per unit resolution volume V_w. It is computed as the sum of all individual scatterers RCS within the volume

$$\sigma_w = \sum_{i=1}^{N} \sigma_i \tag{9.13}$$

where N is the total number of scatterers within the resolution volume. Thus, the total RCS of a single resolution volume is

$$\sigma_W = \sum_{i=1}^{N} \sigma_i V_W \tag{9.14}$$

A resolution volume is shown in Fig. 9.6 and is approximated by

$$V_W \approx \frac{\pi}{8} \theta_a \theta_e R^2 c\tau \tag{9.15}$$

where θ_a and θ_e are, respectively, the antenna azimuth and elevation beamwidths in radians, τ is the pulse width in seconds, c is the speed of light, and R is range.

Consider a propagation medium with an index of refraction m. The ith rain droplet RCS approximation in this medium is

$$\sigma_i \approx \frac{\pi^5}{\lambda^4} K^2 D_i^6 \tag{9.16}$$

where

$$K^2 = \left| \frac{m^2 - 1}{m^2 + 2} \right|^2 \tag{9.17}$$

and D_i is the ith droplet diameter. For example, temperatures between $32°F$ and $68°F$ yield

$$\sigma_i \approx 0.93 \frac{\pi^5}{\lambda^4} D_i^6 \tag{9.18}$$

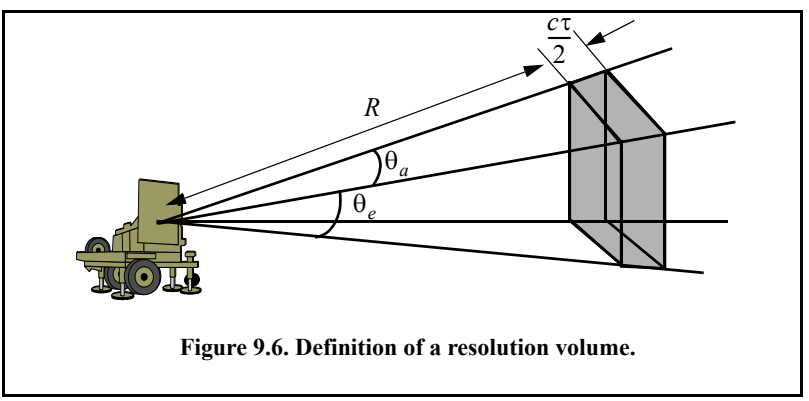

Figure 9.6. Definition of a resolution volume.

and for ice Eq. (9.18) can be approximated by

$$\sigma_i \approx 0.2\frac{\pi^5}{\lambda^4}D_i^6 \tag{9.19}$$

Substituting Eq. (9.19) into Eq. (9.14) yields

$$\sigma_w = \frac{\pi^5}{\lambda^4}K^2 Z \tag{9.20}$$

where the weather clutter coefficient Z is defined as

$$Z = \sum_{i=1}^{N} D_i^6 \tag{9.21}$$

In general, a rain droplet diameter is given in millimeters and the radar resolution volume is expressed in cubic meters; thus the units of Z are often expressed in $millimeter^6/m^3$.

9.3.1. Radar Equation for Volume Clutter

The radar equation gives the total power received by the radar from a σ_t target at range R as

$$S_t = \frac{P_t G^2 \lambda^2 \sigma_t}{(4\pi)^3 R^4} \tag{9.22}$$

where all parameters in Eq. (9.22) have been defined earlier. The weather clutter power received by the radar is

$$S_w = \frac{P_t G^2 \lambda^2 \sigma_w}{(4\pi)^3 R^4} \tag{9.23}$$

It follows that

$$S_w = \frac{P_t G^2 \lambda^2}{(4\pi)^3 R^4}\ \frac{\pi}{8} R^2 \theta_a \theta_e c\tau \sum_{i=1}^{N} \sigma_i \tag{9.24}$$

The SCR for weather clutter is then computed by dividing Eq. (9.22) by Eq. (9.24). More precisely,

$$(SCR)_V = \frac{S_t}{S_w} = (8\sigma_t) \Big/ \left(\pi \theta_a \theta_e c\tau R^2 \sum_{i=1}^{N} \sigma_i \right) \tag{9.25}$$

where the subscript V is used to denote volume clutter.

Example:

A certain radar has target RCS $\sigma_t = 0.1m^2$, *pulse width* $\tau = 0.2\mu s$, *antenna beamwidth* $\theta_a = \theta_e = 0.02 radians$. *Assume the detection range to be* $R = 50Km$, *and compute the SCR if* $\sum \sigma_i = 1.6 \times 10^{-8}(m^2/m^3)$.

Solution:

From Eq. (9.25) we have

$$(SCR)_V = \frac{8\sigma_t}{\pi\theta_a\theta_e c\tau R^2 \sum_N \sigma_i}$$

Substituting the proper values we get

$$(SCR)_V = \frac{(8)(0.1)}{\pi(0.02)^2(3\times10^8)(0.2\times10^{-6})(50\times10^3)^2(1.6\times10^{-8})} = 0.265$$

$$(SCR)_V = -5.76dB.$$

9.4. Clutter RCS

9.4.1. Single Pulse - Low PRF Case

Again the received power from clutter is also calculated using Eq. (9.9). However, in this case the clutter RCS σ_c is computed differently. It is

$$\sigma_c = \sigma_{MBc} + \sigma_{SLc} \qquad \textbf{(9.26)}$$

where σ_{MBc} is the main-beam clutter RCS and σ_{SLc} is the sidelobe clutter RCS, as illustrated in Fig. 9.7.

In order to calculate the total clutter RCS given in Eq. (9.11), one must first compute the corresponding clutter areas for both the main beam and the sidelobes. For this purpose, consider the geometry shown in Fig. 9.8. The angles θ_A *and* θ_E represent the antenna 3-dB azimuth and elevation beamwidths, respectively. The radar height (from the ground to the phase center of the antenna) is denoted by h_r, while the target height is denoted by h_t. The radar slant range is R, and its ground projection is R_g. The range resolution is ΔR and its ground projection is ΔR_g. The main beam clutter area is denoted by A_{MBc} and the sidelobe clutter area is denoted by A_{SLc}.

From Fig. 9.8, the following relations can be derived

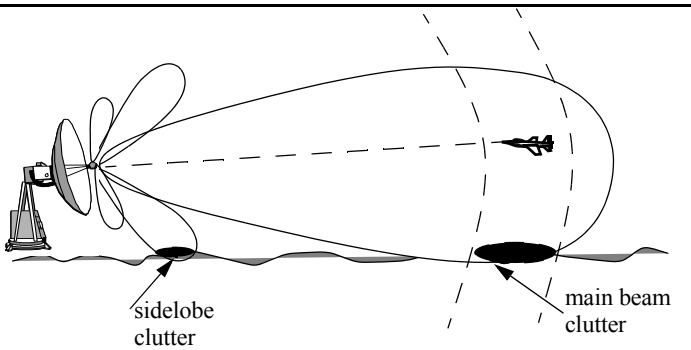

Figure 9.7. Geometry for ground based radar clutter

$$\theta_r = \text{asin}(h_r/R) \tag{9.27}$$

$$\theta_e = \text{asin}((h_t - h_r)/R) \tag{9.28}$$

$$\Delta R_g = \Delta R \cos\theta_r \tag{9.29}$$

where ΔR is the radar range resolution. The slant range ground projection is

$$R_g = R\cos\theta_r \tag{9.30}$$

It follows that the main beam and the sidelobe clutter areas are

$$A_{MBc} = \Delta R_g \; R_g \; \theta_A \tag{9.31}$$

$$A_{SLc} = \Delta R_g \; \pi R_g \tag{9.32}$$

Assume a radar antenna beam $G(\theta)$ of the form

$$G(\theta) = \exp\left(-\frac{2.776\theta^2}{\theta_E^2}\right) \Rightarrow Gaussian \tag{9.33}$$

$$G(\theta) = \left\{ \begin{array}{ll} \left(\dfrac{\sin\left(\dfrac{\theta}{\theta_E}\right)}{\left(\dfrac{\theta}{\theta_E}\right)}\right)^2 & ;|\theta| \le \dfrac{\pi\theta_E}{2.78} \\ 0 & ;elsewhere \end{array} \right\} \Rightarrow \left(\frac{\sin(x)}{x}\right)^2 \tag{9.34}$$

Then the main-beam clutter RCS is

$$\sigma_{MBc} = \sigma^0 A_{MBc} G^2(\theta_e + \theta_r) = \sigma^0 \Delta R_g \; R_g \; \theta_A G^2(\theta_e + \theta_r) \tag{9.35}$$

and the sidelobe clutter RCS is

$$\sigma_{SLc} = \sigma^0 A_{SLc} (SL_{rms})^2 = \sigma^0 \Delta R_g \; \pi R_g (SL_{rms})^2 \tag{9.36}$$

where the quantity SL_{rms} is the rms for the antenna sidelobe level.

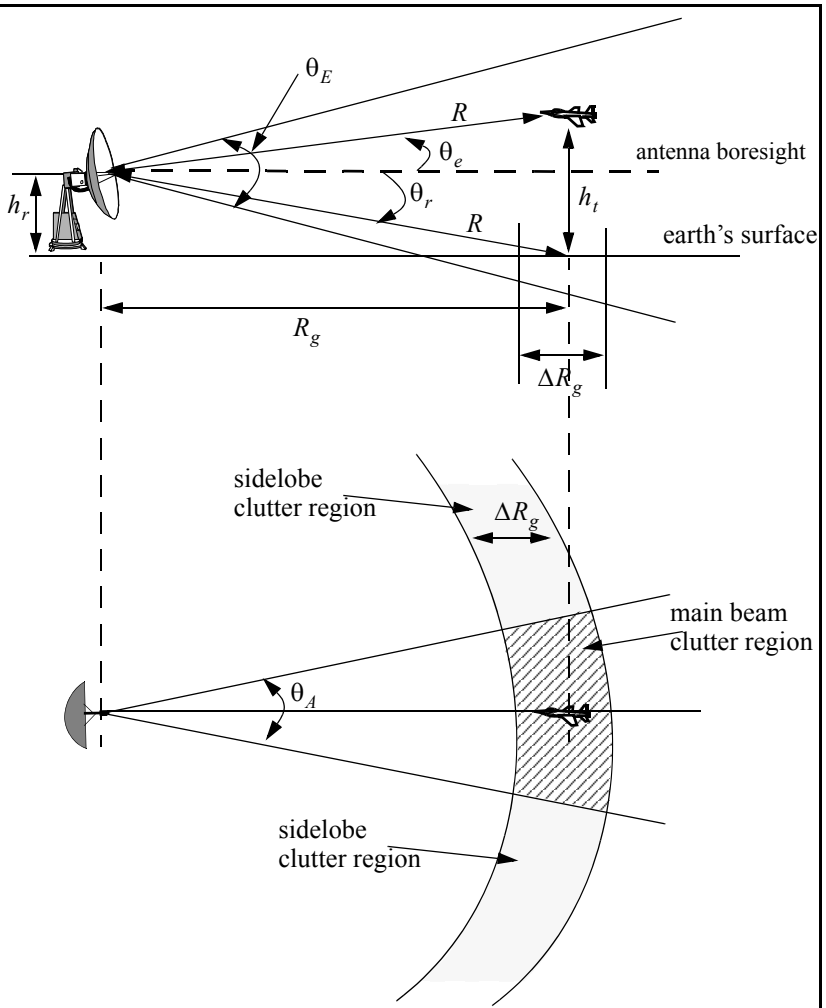

Figure 9.8. Clutter geometry for ground based radar. Side view and top view.

Finally, in order to account for the variation of the clutter RCS versus range, one can calculate the total clutter RCS as a function of range. It is given by

$$\sigma_c(R) = \frac{\sigma_{MBc} + \sigma_{SLc}}{(1 + (R/R_h)^4)} \tag{9.37}$$

where R_h is the radar range to the horizon calculated as

$$R_h = \sqrt{8 h_r r_e / 3} \tag{9.38}$$

where r_e is the Earth's radius equal to $6371 Km$. The denominator in Eq. (9.37) is put in that format in order to account for refraction and for round (spherical) Earth effects.

The radar SNR due to a target at range R is

$$SNR = \frac{P_t G^2 \lambda^2 \sigma_t}{(4\pi)^3 R^4 k T_o B F L} \tag{9.39}$$

where, as usual, P_t is the peak transmitted power, G is the antenna gain, λ is the wavelength, σ_t is the target RCS, k is Boltzmann's constant, T_0 is the effective noise temperature, B is the radar operating bandwidth, F is the receiver noise figure, and L is the total radar losses. Similarly, the Clutter-to-Noise Ratio (CNR) at the radar is

$$CNR = \frac{P_t G^2 \lambda^2 \sigma_c}{(4\pi)^3 R^4 k T_o B F L} \tag{9.40}$$

where the σ_c is calculated using Eq. (9.37).

When the clutter statistic is Gaussian, the clutter signal return and the noise return can be combined, and a new value for determining the radar measurement accuracy is derived from the Signal-to-Clutter+Noise Ratio, denoted by SIR. It is given by

$$SIR = \frac{SNR}{1 + CNR} \tag{9.41}$$

Note that the CNR is computed from Eq. (9.40).

9.4.2. High PRF Case

High PRFs are typically used by pulsed Doppler radars. Pulsed Doppler radars use very short unmodulated train of pulses, and hence, range resolution is limited by the pulsewidth, which forces the radar to use extremely short duration pulses. High PRF radars make up for the loss of average transmitted power due to using short pulses by coherently processing a train of these pulses

within one coherent processing interval (integration time or dwell interval). Although high PRF radars although are ambiguous in range, they provide excellent capability to measuring Doppler frequency. Range ambiguity can be dealt with by using multiple PRF (PRF staggering) which will be addressed later section. One major drawback of using high PRFs (or pulsed Doppler radars) is the fact that pulsed Doppler radars have to contend with much more clutter than do low PRF radars.

Consider the illustrations shown in Fig. 9.9. The low PRF case is shown in Fig. 9.9a. In this case, the target is at maximum detection range which corresponds to an unambiguous range

$$R_u = \frac{cT}{2} = \frac{c}{2f_r} \tag{9.42}$$

where T is the pulse repetition interval and f_r is the radar PRF. The amount of clutter entering the radar through its main-beam corresponds only to the clutter patch located at the target's range. Alternatively, in Fig. 9.9b the high PRF case is depicted. In this case, the radar is range ambiguous and the amount of main-beam clutter entering the radar corresponds to many more clutter patches as shown in Fig. 9.9b. Consequently, the amount of clutter competing with target detection in an order of magnitude larger than the case of low PRF. This is typically referred to as clutter folding.

Denote the clutter power entering the radar due to a single pulse for the target at range R_0 as P_{C_1}, then because of the high PRF operation, the total clutter power entering the radar is

$$P_{C_{folded}} = \sum_{n=0}^{N-1} P_{C_1} Rect\left(\frac{t-nT}{\tau_0}\right) \tag{9.43}$$

where N is the number of pulses in one coherent processing interval (dwell), T is the PRI, and τ_0 is the pulsewidth. Note that since the radar receiver is shut off during transmission of a given pulse, Eq. (9.43) is computed only at delays (range) that correspond to

$$\{(nT + 2\tau_0) < t < (n+1)T - \tau_0;\ \ 0 \le n \le N-1\} \tag{9.44}$$

where in this case, the transmitter is assumed to be shut off not only during the transmission of each pulse but also for one pulsewidth before and after each transmission. Thus, one would expect the folded clutter RCS to not be continuous versus the range, but rather to exist over intervals of length T seconds with gaps that correspond to three times the pulsewidth. This is illustrated in the following few examples for both low and high PRF cases.

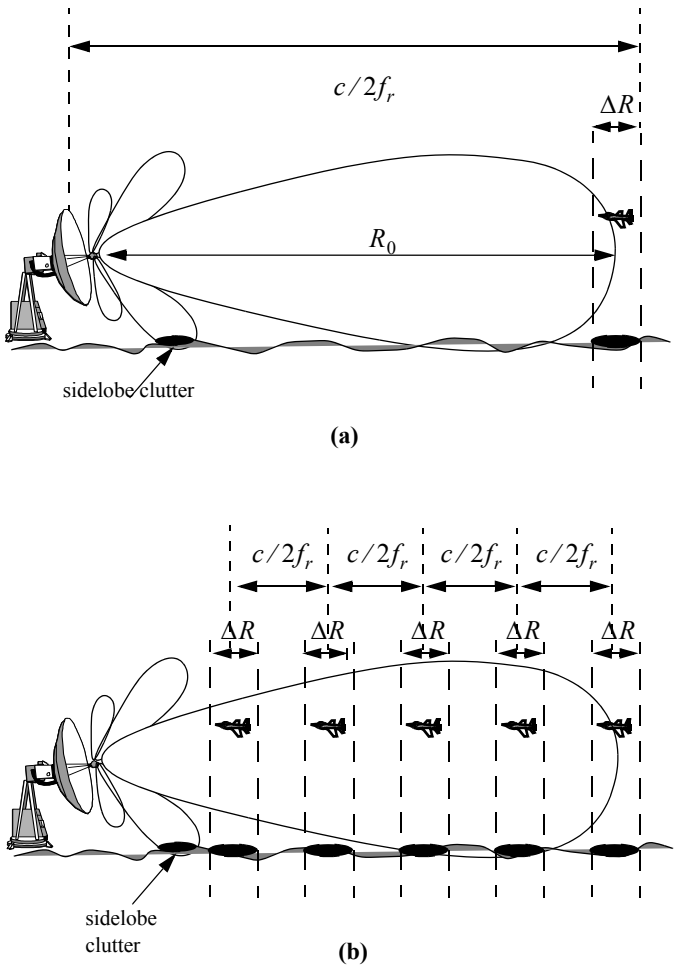

Figure 9.9. Mainbeam clutter entering radar. (a) Low PRF case; (b) high PRF case.

As an example consider the case with the following parameters

clutter back scatterer coefficient	*-20 dB*
antenna 3dB elevation beamwidth	*1.5 degrees*
antenna 3dB azimuth beamwidth	*2 degrees*
antenna sidelobe level	*-25 dB*
radar height	*3 meters*

target height	150 meters
radar peak power	45 KW
radar operating frequency	50 KHz
pulsewidth	1 micro sec
effective noise temperature	290 Kelvins
noise figure	6 dB
radar losses	10 dB
target RCS	-10 dBsm
radar center frequency	5 GHz

Figure 9.10 is concerned with a low PRF case (i.e, single pulse, no clutter folding). Figure 9.10a shows the clutter RCS versus range when a sin(x)/x antenna pattern is used, and Fig. 9.10b shows the resulting SNR, CNR, and SCR. Figure 9.11 is similar to Fig. 9.10 except in this case the antenna has a Gaussian shape. These plots can be reproduced using the following MATLAB code which uses the function *"clutter_rcs.m."*

```
%Use this code to generate Fig. 9.10 and 9.11
clear all;
close all;
k = 1.38e-23; % Boltzman's constant
pt = 45e3;
theta_AZ = 1.5;
theta_EL = 2;
F = 6;
L = 10;
tau = 1e-6;
B = 1/tau;
sigmmat = -10;
sigmma0 = -20;
SL = -25;
hr = 3;
ht = 150;
f0 = 5e9;
lambda = 3e8/f0;
range = linspace(2,50, 120);
[sigmmaC] = clutter_rcs(sigmma0, theta_EL, theta_AZ, SL, range, hr, ht, B,1);
sigmmaC = 10.^(sigmmaC./10);
range_m = 1000 .* range;
F = 10.^(F/10); % noise figure is 6 dB
T0 = 290; % noise temperature 290K
g = 26000 /theta_AZ /theta_EL; % antenna gain
Lt = 10.^(L/10); % total radar losses 13 dB
sigmmat = 10^(sigmmat/10)
```

```
CNR = pt*g*g*lambda^2 .* sigmmaC ./ ((4*pi)^3 .* (range_m).^4 .* k*T0*F*Lt*B); %
CNR
SNR = pt*g*g*lambda^2 .* sigmmat ./ ((4*pi)^3 .* (range_m).^4 .* k*T0*F*L*B); %
SNR
SCR = SNR ./ CNR; % Signal to clutter ratio
SIR = SNR ./ (1+CNR); % Signal to interference ratio
%%%%%%%%%%%%%%%%%%%%%%%%%%%%%%%%%%%%
figure(2)
subplot(3,1,1)
plot(range,10*log10(SNR));
ylabel('SNR in dB');
grid on;
axis tight
subplot(3,1,2)
plot(range,10*log10(CNR));
ylabel('CNR in dB');
grid on;
axis tight
subplot(3,1,3)
plot(range,10*log10(SCR));
ylabel('SCR in dB') ;
grid on;
axis tight
xlabel('Range in Km')
```

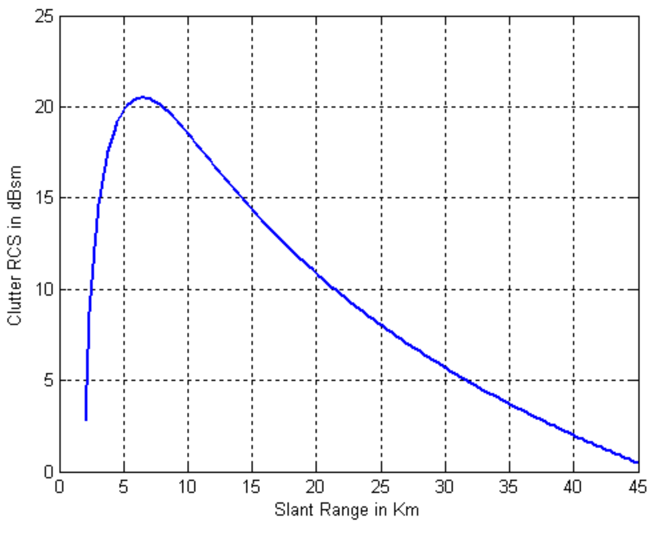

Figure 9.10a. Clutter RCS versus range with sin(x)/x antenna pattern. Single pulse case.

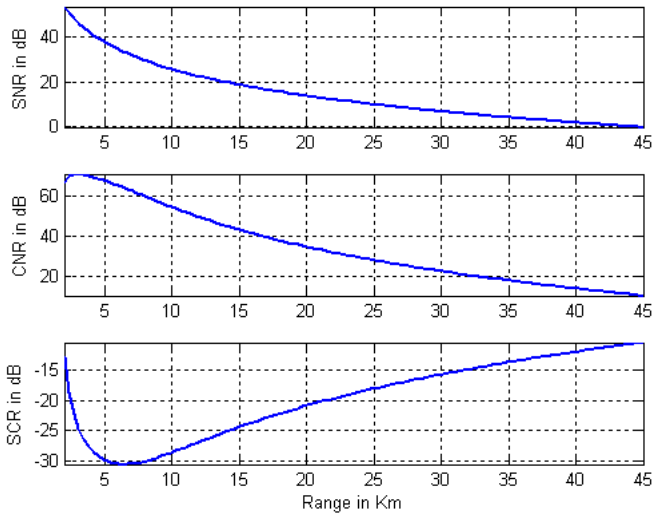

Figure 9.10b. SNR, CNR, and SCR corresponding to Fig. 9.10a.

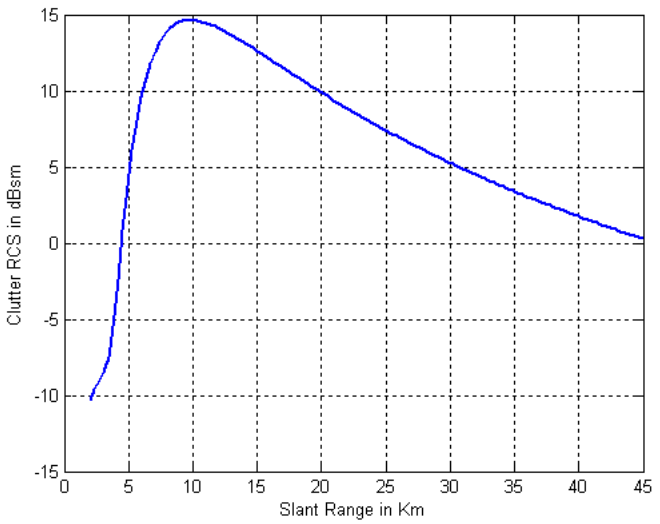

Figure 9.11a. Clutter RCS versus range with Gaussian antenna pattern. Single pulse case.

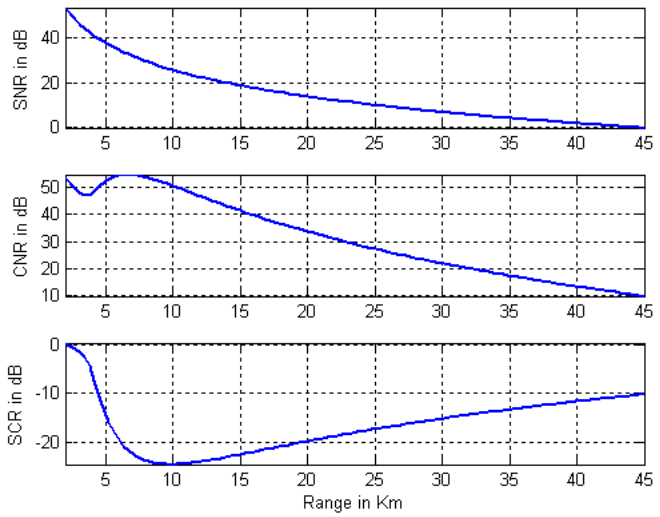

Figure 9.11b. SNR, CNR, and SCR corresponding to Fig. 9.11a.

Figure 9.12 shows the SNR, CNR, and SCR for the high PRF case (i.e, pulse Doppler radar, clutter folding). In this figure the antenna pattern has a sin(x)/x shape. Figure 9.13 is similar to Fig. 9.12 except in this case the antenna pattern is Gaussian. These plots can be reproduced using the following MATLAB code.

```
% Use this code to generate Fig. 9.12 or 9. 13 of text
clear all
close all
k = 1.38e-23; % Boltzmann's constant
T0 = 290; % degrees Kelvin
ant_id = 1; % use 1 for sin(x)/x antenna pattern and use 2 for Gaussian pattern
theta_ref = 0.75; % reference angle of radar antenna in degrees
re = 6371000 * 4 /3; % 4/3rd earth radius in Km
c = 3e8; % speed of light
theta_EL = 1.5; % Antenna elevation beamwidth in degrees
theta_AZ = 2.; % Antenna azimuth beamwidth in degrees
SL_dB = -25; % Antenna RMS sidelobe level
hr = 3; % Radar antenna height in meters
ht = 150; % Target height in meters
Sigmmat = -10; % Target RCS in dB
Sigmma0 = -20; % Clutter backscatter coefficient
P = 45e3; % Radar peak power in Watts
tau = 1e-6; % Pulse width (unmodulated)
```

```
fr = 50e3; % PRF in Hz
f0 = 5e9; % Radar center frequency
F = 6; % Noise figure in dB
L = 10; % Radar losses in dB
lambda = c /f0;
SL = 10^(SL_dB/10);
sigmma0 = 10^(Sigmma0/10);
F = 10^(F/10);
L = L^(L/10);
sigmmat = 10^(Sigmmat/10);
T = 1/fr; % PRI
B = 1/tau; % Bandwidth
delr = c * tau /2; % Range resolution;
Rh = sqrt(2*re*hr); % Range to Horizon
R1 = [2*delr:delr:c/2*(T-tau)];
Rclut = sqrt(R1.^2 + hr^2); % Range to clutter patches
G = 26000 /theta_EL /theta_AZ; % Antenna gain
for j = 0:40
   Rtgt = [c/2*(j*T+2*tau):delr:c/2*((j+1)*T-tau)];
   thetaR = asin(hr./Rclut); % Ele angle from radar to clutter patch target is present
   thetae = theta_ref *pi/180;
   d = Rclut .* cos(thetaR); % Ground range to center of clutter at range Rclut
   del_d = delr .* cos(thetaR);
   % claculte clutter RCS
   theta_sum = thetaR+thetae;
   if(ant_id ==1) % use sinc^2 antenna pattern
      ant_arg = ( theta_sum ) ./ (pi*theta_EL/180);
      gain = (sinc(ant_arg)).^2;
   else
      gain = exp(-2.776 .*(theta_sum./(pi*theta_EL/180)).^2);
   end
   % clutter RCS
    sigmmac = (pi*SL^2+(theta_AZ*pi/180).*gain.*sigmma0.*d.*del_d) ./ (1+(Rclut/
Rh).^4);
    CNR = P*G*G*lambda^2 .* sigmmac ./ ((4*pi)^3 .* Rclut.^4 .* k*T0*F*L*B); %
CNR
   SNR = P*G*G*lambda^2 .* sigmmat ./ ((4*pi)^3 .* Rtgt.^4 .* k*T0*F*L*B); % SNR
   SCR = SNR ./ CNR; % Signal to clutter ratio
   SIR = SNR ./ (1+CNR); % Signal to interfernce ratio
   figure(2)
   subplot(4,1,1),
   hold on
   plot(Rtgt/1000,10*log10(SNR));
   ylabel('SNR - dB');
  grid on
  subplot(4,1,2),
  hold on
   plot(Rtgt/1000,10*log10(CNR));
```

```
    ylabel('CNR - dB');
    grid on
    subplot(4,1,3),
    hold on
    plot(Rtgt/1000,10*log10(SCR));
    ylabel('SCR - dB') ;
    grid on
    subplot(4,1,4),
    hold on
    plot(Rtgt/1000,10*log10(SIR));
    xlabel('Range - Km')
    ylabel('SIR - dB');
   grid on
end
subplot(4,1,1)
axis([0 50 -10 100])
subplot(4,1,2)
axis([0 50 60 90]);
subplot(4,1,3)
axis([0 50 -100 0])
subplot(4,1,4)
axis([0 50 -100 0])
```

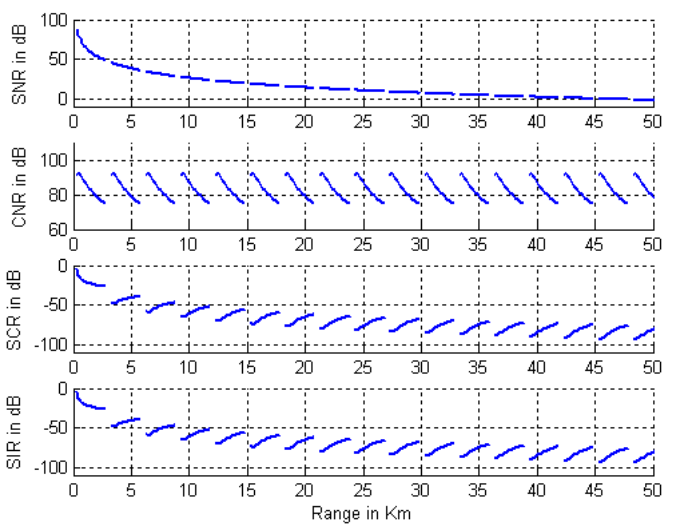

Figure 9.12. SIR, SCR, CNR, and SNR for a pulse Doppler radar with sin(x)/x antenna pattern.

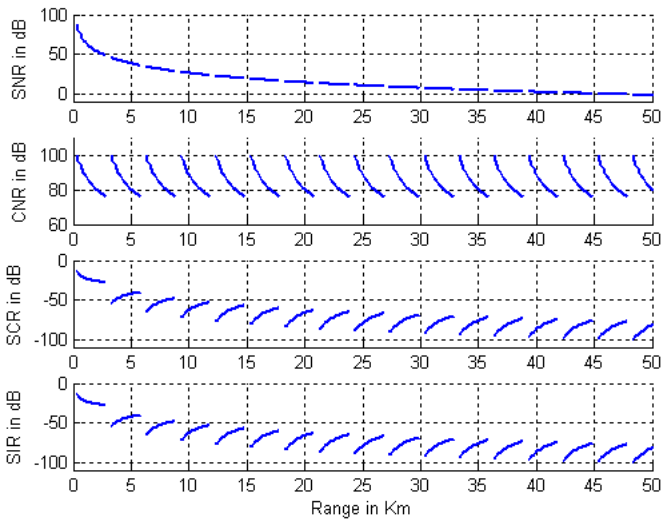

Figure 9.13. SIR, SCR, CNR, and SNR for a pulse Doppler radar with Gaussian antenna pattern.

9.5. Clutter Spectrum

9.5.1. Clutter Statistical Models

Since clutter within a resolution cell or volume is composed of a large number of scatterers with random phases and amplitudes, it is statistically described by a probability distribution function. The type of distribution depends on the nature of clutter itself (sea, land, volume), the radar operating frequency, and the grazing angle.

If sea or land clutter is composed of many small scatterers when the probability of receiving an echo from one scatterer is statistically independent of the echo received from another scatterer, then the clutter may be modeled using a Rayleigh distribution,

$$f(x) = \frac{2x}{x_0}\exp\left(\frac{-x^2}{x_0}\right) \quad ; \quad x \geq 0 \tag{9.45}$$

where x_0 is the mean-squared value of x.

The log-normal distribution best describes land clutter at low grazing angles. It also fits sea clutter in the plateau region. It is given by

$$f(x) = \frac{1}{\sigma\sqrt{2\pi}\ x}\ \exp\left(-\frac{(\ln x - \ln x_m)^2}{2\sigma^2}\right)\ ;\ x > 0 \qquad \textbf{(9.46)}$$

where x_m is the median of the random variable x, and σ is the standard deviation of the random variable $\ln(x)$.

The Weibull distribution is used to model clutter at low grazing angles (less than five degrees) for frequencies between 1 and $10GHz$. The Weibull probability density function is determined by the Weibull slope parameter a (often tabulated) and a median scatter coefficient $\bar{\sigma}_0$, and is given by

$$f(x) = \frac{bx^{b-1}}{\bar{\sigma}_0}\ \exp\left(-\frac{x^b}{\bar{\sigma}_0}\right);\ x \geq 0 \qquad \textbf{(9.47)}$$

where $b = 1/a$ is known as the shape parameter. Note that when $b = 2$ the Weibull distribution becomes a Rayleigh distribution.

9.5.2. Clutter Components

It was established earlier that the complex envelope of the signal received by the radar comprise the target returns and additive bandlimited white noise. In the presence of clutter, the complex envelope is now composed of target, noise, and clutter returns. That is,

$$\tilde{x}(t) = \tilde{s}(t) + \tilde{n}(t) + \tilde{w}(t) \qquad \textbf{(9.48)}$$

where $\tilde{s}(t)$, $\tilde{n}(t)$, and $\tilde{w}(t)$ are, respectively, the target, noise, and clutter complex envelope echoes. Noise is typically modeled (as discussed in earlier chapters) as a bandlimited white Gaussian random process. Furthermore, noise samples are consider statistically independent of each other and of clutter measurements.

Clutter arises from reflections of unwanted objects within the radar beam. Since many objects comprose the clutter returns, clutter may also be molded as a Gaussian random process. In other words, clutter samples from one radar measurement to another constitute a joint set of Gaussian random variables. However, because of the clutter fluctuation and due to antenna mechanical scanning, wind speed, and radar platform motion (if applicable), these random variables are not statistically independent.

More precisely, because of the antenna mechanical scanning, clutter returns in the radar mainbeam do not have the same amplitude from pulse to pulse. This will effectively add amplitude modulation to the clutter returns. This additional modulation is governed by the shape of the antenna pattern, the rate of mechanical scanning, and the radar PRF. Denote the antenna two-way azimuth $3dB$ beamwidth as θ_a and the antenna scan rate as $\dot{\theta}_{scan}$. It follows that the

contribution of antenna scanning to the standard deviation of the clutter fluctuation is

$$\sigma_s = 0.399\frac{\dot{\theta}_{scan}}{\theta_a} \tag{9.49}$$

Another contributor to the clutter spectral spreading is caused by motion of the clutter itself, due to wind. Trees, vegetation, and sea waves are the main contributors to this effect. This relative motion, although relatively small, introduces additional Doppler shift in the clutter returns. Earlier, it was established that Doppler frequency due to a relative velocity v is given by

$$f_d = 2v/\lambda \tag{9.50}$$

where λ is the radar operating wavelength. It follows that if the apparent rms velocity due to wind is v_{rms}, then the standard deviation is

$$\sigma_w = 2v_{rms}/\lambda \tag{9.51}$$

Finally, if the radar platform is in motion, then the relative motion between the platform and the stationary clutter will cause a Doppler shift given by

$$f_c = (2v_{radar}\cos\theta)/\lambda \tag{9.52}$$

where $v_{radar}\cos\theta$ is the radial velocity component of the platform in the direction of clutter. Since the radar beam has a finite width, not all clutter components have the same radial velocity at all times. More specifically, if the angles θ_1 and θ_2 represent the edges of the radar beam, then Eq. (9.52) ca be written as

$$f_c = \frac{2v_{radar}}{\lambda}(\cos\theta_2 - \cos\theta_1) \approx \frac{2v_{radar}}{\lambda}\theta_a \sin\theta \tag{9.53}$$

and the standard deviation due to platform motion is given by

$$\sigma_v = \frac{v_{radar}}{\lambda}\sin\theta \tag{9.54}$$

Finally, the overall clutter spreading is denoted by σ_f, where

$$\sigma_f^2 = \sigma_v^2 + \sigma_s^2 + \sigma_w^2 \tag{9.55}$$

The overall value of the clutter spreading defined in Eq. (9.55) is relatively small.

9.5.3. Clutter Power Spectrum Density

Clutter primarily comprises stationary ground unwanted reflections with limited relative motion with respect to the radar. Therefore, its power spectrum density will be concentrated around $f = 0$. However, because σ_f (see Eq. (9.55)) is not always zero, clutter actually exhibits some Doppler frequency spread. The clutter power spectrum can be written as the sum of fixed (stationary) and random (due to frequency spreading) components, as

$$S_c(f) = \frac{P_c}{T\sigma_f\sqrt{2\pi}} \sum_{k=-\infty}^{\infty} \exp\left(-\frac{(f-k/T)^2}{2\sigma_f^2}\right) \tag{9.56}$$

where T is the PRI (i.e., $1/f_r$, f_r is the PRF), P_c is the clutter power or clutter mean square value, and σ_f is the clutter spectral spreading parameter as defined in Eq. (9.55). As clearly indicated by Eq. (9.56), the clutter PSD is periodic with period equal to f_r. Furthermore, the clutter PSD extends about each multiple integer of the PRF in accordance with Eq. (9.55). It must be noted that this spread is relatively small and thus the relation $\sigma_f \ll f_r$ is always true. This is illustrated in Fig. 9.14. The mean square value can be calculated from

$$P_c = T \int_{-f_r/2}^{f_r/2} S_c(f)df \tag{9.57}$$

Let $S_{c0}(f)$ denote the central portion of Eq. (9.56); then P_c is be expressed by

$$P_c = T \int_{-\infty}^{\infty} S_{c0}(f)df \tag{9.58}$$

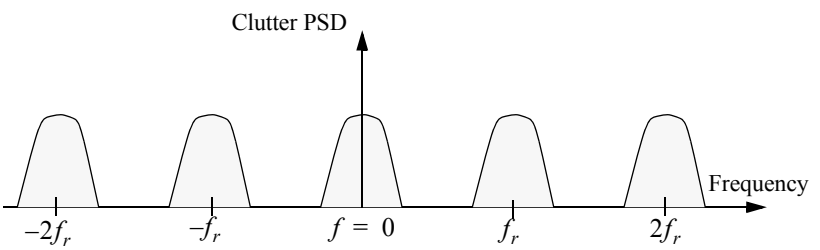

Figure 9.14. Typical clutter PSD.

where $S_{c0}(f)$ is a Gaussian shape function given by

$$S_{c0}(f) = \frac{k}{\sigma_f\sqrt{2\pi}} \exp\left(-\frac{f^2}{2\sigma_f^2}\right) \tag{9.59}$$

and $k = P_c/T$.

9.6. Moving Target Indicator (MTI)

The clutter spectrum is concentrated around DC ($f = 0$) and multiple integers of the radar PRF f_r, as was illustrated in Fig. 9.14. In CW radars, clutter is avoided or suppressed by ignoring the receiver output around DC, since most of the clutter power is concentrated about the zero frequency band. Pulsed radar systems may utilize special filters that can distinguish between slow-moving or stationary targets and fast-moving ones. This class of filter is known as the Moving Target Indicator (MTI). In simple words, the purpose of an MTI filter is to suppress target-like returns produced by clutter and allow returns from moving targets to pass through with little or no degradation. In order to effectively suppress clutter returns, an MTI filter needs to have a deep stop-band at DC and at integer multiples of the PRF. Figure 9.15b shows a typical sketch of an MTI filter response, while Fig. 9.15c shows its output when the PSD shown in Fig. 9.15a is the input.

MTI filters can be implemented using delay line cancelers. As we will show later in this chapter, the frequency response of this class of MTI filter is periodic, with nulls at integer multiples of the PRF. Thus, targets with Doppler frequencies equal to nf_r are severely attenuated. Since Doppler is proportional to target velocity ($f_d = 2v/\lambda$), target speeds that produce Doppler frequencies equal to integer multiples of f_r are known as blind speeds. More precisely,

$$v_{blind} = (n\lambda f_r)/2; \quad n \geq 0 \tag{9.60}$$

Radar systems can minimize the occurrence of blind speeds either by employing multiple PRF schemes (PRF staggering) or by using high PRFs in which the radar may become range ambiguous. The main difference between PRF staggering and PRF agility is that the pulse repetition interval (within an integration interval) can be changed between consecutive pulses for the case of PRF staggering.

9.6.1. Single Delay Line Canceler

A single delay line canceler can be implemented as shown in Fig. 9.16. The canceler's impulse response is denoted as $h(t)$. The output $y(t)$ is equal to the convolution between the impulse response $h(t)$ and the input $x(t)$. The single delay canceler is often called a two-pulse canceler since it requires two distinct input pulses before an output can be read.

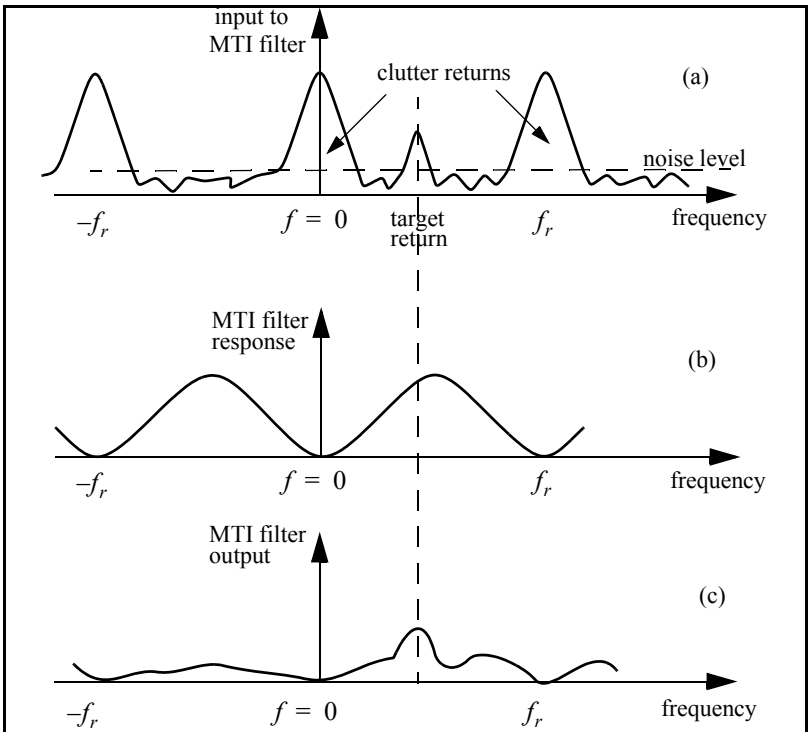

Figure 9.15. (a) Typical radar return PSD when clutter and target are present. (b) MTI filter frequency response. (c) Output from an MTI filter.

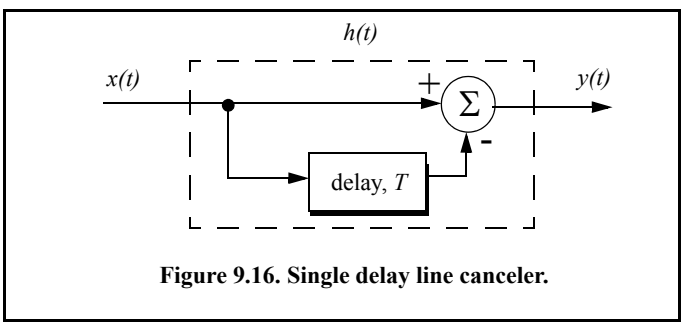

Figure 9.16. Single delay line canceler.

The delay T is equal to the radar PRI ($1/f_r$). The output signal $y(t)$ is

$$y(t) = x(t) - x(t - T) \tag{9.61}$$

The impulse response of the canceler is given by

$$h(t) = \delta(t) - \delta(t - T) \tag{9.62}$$

where $\delta(\ )$ is the delta function. It follows that the Fourier transform (FT) of $h(t)$ is

$$H(\omega) = 1 - e^{-j\omega T} \tag{9.63}$$

where $\omega = 2\pi f$. In the z-domain, the single delay line canceler response is

$$H(z) = 1 - z^{-1} \tag{9.64}$$

The power gain for the single delay line canceler is given by

$$|H(\omega)|^2 = H(\omega)H^*(\omega) = (1 - e^{-j\omega T})(1 - e^{j\omega T}) \tag{9.65}$$

It follows that

$$|H(\omega)|^2 = 1 + 1 - (e^{j\omega T} + e^{-j\omega T}) = 2(1 - \cos\omega T) \tag{9.66}$$

and using the trigonometric identity $(2 - 2\cos 2\vartheta) = 4(\sin\vartheta)^2$ yields

$$|H(\omega)|^2 = 4(\sin(\omega T/2))^2 \tag{9.67}$$

The amplitude frequency response for a single delay line canceller is shown in Fig. 9.17. Clearly, the frequency response of a single canceler is periodic with a period equal to f_r. The peaks occur at $f = (2n + 1)/(2f_r)$, and the nulls are at $f = nf_r$, where $n \geq 0$. In most radar applications the response of a single canceler is not acceptable since it does not have a wide notch in the stop-band. A double delay line canceler has better response in both the stop- and pass-bands, and thus it is more frequently used than a single canceler. In this book, we will use the names *single delay line canceler* and *single canceler* interchangeably.

9.6.2. Double Delay Line Canceler

Two basic configurations of a double delay line canceler are shown in Fig. 9.18. Double cancelers are often called three-pulse cancelers since they require three distinct input pulses before an output can be read. The double line canceler impulse response is given by

$$h(t) = \delta(t) - 2\delta(t - T) + \delta(t - 2T) \tag{9.68}$$

Again, the names *double delay line canceler* and *double canceler* will be used interchangeably. The power gain for the double delay line canceler is

$$|H(\omega)|^2 = |H_1(\omega)|^2 |H_1(\omega)|^2 \tag{9.69}$$

where $|H_1(\omega)|^2$ is the single line canceler power gain given in Eq. (9.55). It follows that

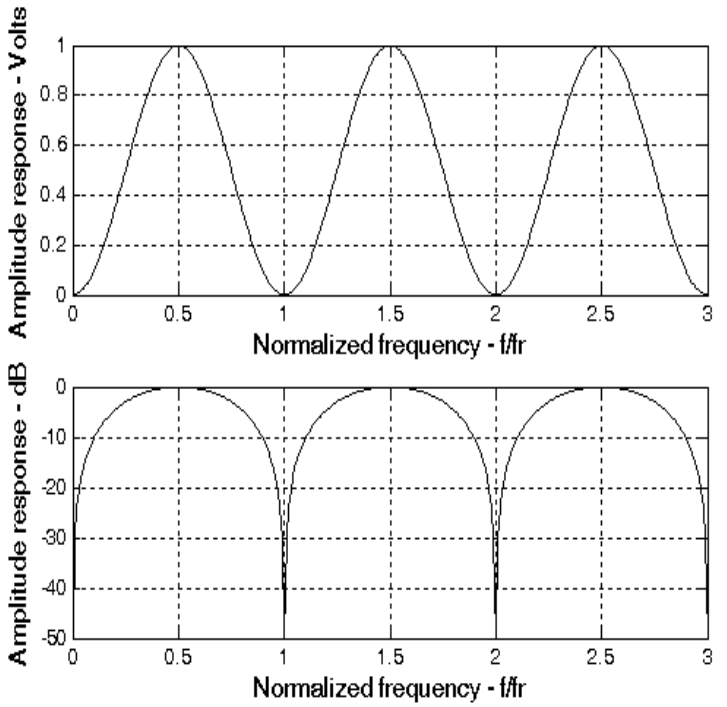

Figure 9.17. Single canceler frequency response.

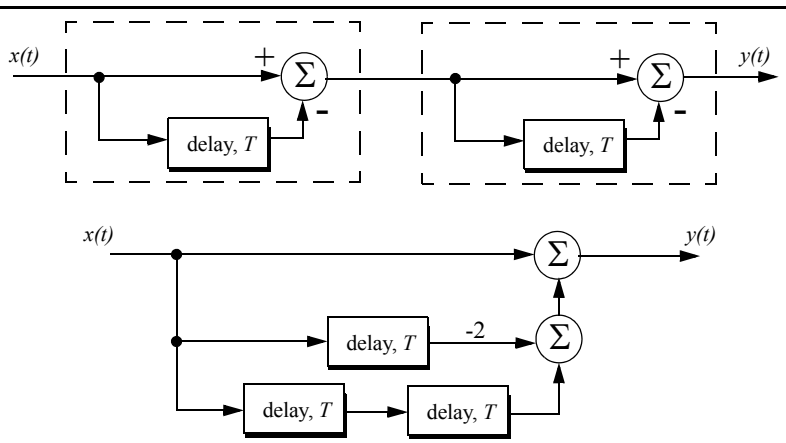

Figure 9.18. Two configurations for a double delay line canceler.

$$|H(\omega)|^2 = 16\left(\sin\left(\omega\frac{T}{2}\right)\right)^4 \tag{9.70}$$

And in the z-domain, we have

$$H(z) = (1-z^{-1})^2 = 1-2z^{-1}+z^{-2} \tag{9.71}$$

Figure 9.19 shows typical output from this function. Note that the double canceler has a better response than the single canceler (deeper notch and flatter pass-band response).

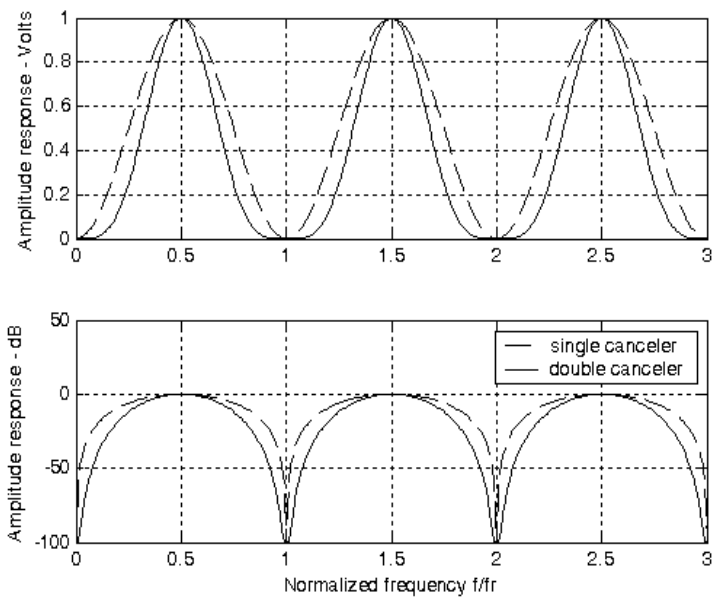

Figure 9.19. Normalized frequency responses for single and double cancelers.

9.6.3. Delay Lines with Feedback (Recursive Filters)

Delay line cancelers with feedback loops are known as recursive filters. The advantage of a recursive filter is that through a feedback loop, we will be able to shape the frequency response of the filter. As an example, consider the single canceler shown in Fig. 9.20. From the figure we can write

$$y(t) = x(t) - (1-K)w(t) \tag{9.72}$$

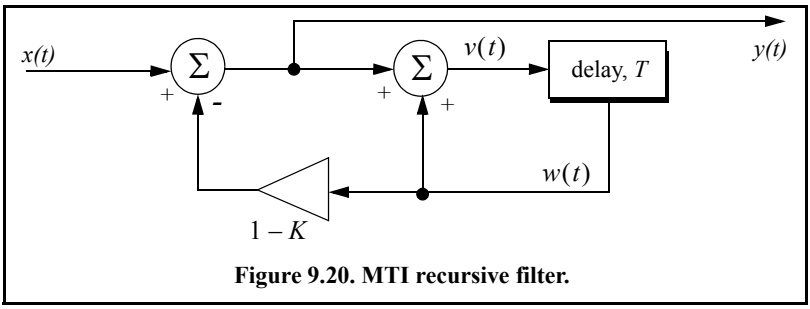

Figure 9.20. MTI recursive filter.

$$v(t) = y(t) + w(t) \tag{9.73}$$

$$w(t) = v(t - T) \tag{9.74}$$

Applying the z-transform to the above three equations yields

$$Y(z) = X(z) - (1 - K)W(z) \tag{9.75}$$

$$V(z) = Y(z) + W(z) \tag{9.76}$$

$$W(z) = z^{-1}V(z) \tag{9.77}$$

Solving for the transfer function $H(z) = Y(z)/X(z)$ yields

$$H(z) = \frac{1 - z^{-1}}{1 - Kz^{-1}} \tag{9.78}$$

The modulus square of $H(z)$ is then equal to

$$|H(z)|^2 = \frac{(1 - z^{-1})(1 - z)}{(1 - Kz^{-1})(1 - Kz)} = \frac{2 - (z + z^{-1})}{(1 + K^2) - K(z + z^{-1})} \tag{9.79}$$

Using the transformation $z = e^{j\omega T}$ yields

$$z + z^{-1} = 2\cos\omega T \tag{9.80}$$

Thus, Eq. (9.79) can now be rewritten as

$$\left|H(e^{j\omega T})\right|^2 = \frac{2(1 - \cos\omega T)}{(1 + K^2) - 2K\cos(\omega T)} \tag{9.81}$$

Note that when $K = 0$, Eq. (9.81) collapses to Eq. (9.67) (single line canceler). Figure 9.21 shows a plot of Eq. (9.81) for $K = 0.25, 0.7, 0.9$. Clearly, by changing the gain factor K one can control the filter response. This plot can be reproduced using the following MATLAB code.

```
clear all;
fofr = 0:0.001:1;
arg = 2.*pi.*fofr;
nume = 2.*(1.-cos(arg));
den11 = (1. + 0.25 * 0.25);
den12 = (2. * 0.25) .* cos(arg);
den1 = den11 - den12;
den21 = 1.0 + 0.7 * 0.7;
den22 = (2. * 0.7) .* cos(arg);
den2 = den21 - den22;
den31 = (1.0 + 0.9 * 0.9);
den32 = ((2. * 0.9) .* cos(arg));
den3 = den31 - den32;
resp1 = nume ./ den1;
resp2 = nume ./ den2;
resp3 = nume ./ den3;
plot(fofr,resp1,'k',fofr,resp2,'k-.',fofr,resp3,'k--');
xlabel('Normalized frequency')
ylabel('Amplitude response')
legend('K=0.25','K=0.7','K=0.9')
grid
axis tight
```

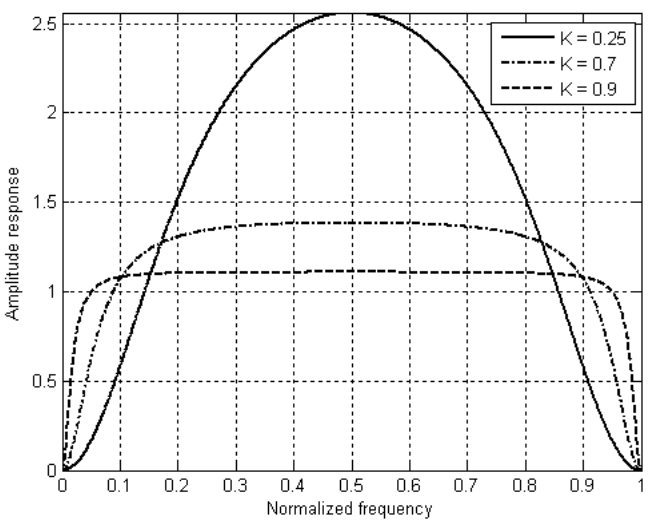

Figure 9.21. Frequency response corresponding to Eq. (9.81).

In order to avoid oscillation due to the positive feedback, the value of K should be less than unity. The value $(1-K)^{-1}$ is normally equal to the number of pulses received from the target. For example, $K = 0.9$ corresponds to ten pulses, while $K = 0.98$ corresponds to about fifty pulses.

9.7. PRF Staggering

Target velocities that correspond to multiple integers of the PRF are referred to as blind speeds. This terminology is used since an MTI filter response is equal to zero at these values. Blind speeds can pose serious limitations on the performance of MTI radars and their ability to perform adequate target detection. Using PRF agility by changing the pulse repetition interval between consecutive pulses can extend the first blind speed to more tolerable values. In order to show how PRF staggering can alleviate the problem of blind speeds, let us first assume that two radars with distinct PRFs are utilized for detection. Since blind speeds are proportional to the PRF, the blind speeds of the two radars would be different. However, using two radars to alleviate the problem of blind speeds is a very costly option. A more practical solution is to use a single radar with two or more different PRFs.

For example, consider a radar system with two interpulse periods T_1 and T_2, such that

$$\frac{T_1}{T_2} = \frac{n_1}{n_2} \tag{9.82}$$

where n_1 and n_2 are integers. The first true blind speed occurs when

$$\frac{n_1}{T_1} = \frac{n_2}{T_2} \tag{9.83}$$

This is illustrated in Fig. 9.22 for $n_1 = 4$ and $n_2 = 5$. The ratio

$$k_s = \frac{n_1}{n_2} \tag{9.84}$$

is known as the stagger ratio. Using staggering ratios closer to unity pushes the first true blind speed farther out. However, the dip in the vicinity of $1/T_1$ becomes deeper. In general, if there are N PRFs related by

$$\frac{n_1}{T_1} = \frac{n_2}{T_2} = \ldots = \frac{n_N}{T_N} \tag{9.85}$$

and if the first blind speed to occur for any of the individual PRFs is v_{blind1}, then the first true blind speed for the staggered waveform is

$$v_{blind} = \frac{n_1 + n_2 + \ldots + n_N}{N} \; v_{blind1} \tag{9.86}$$

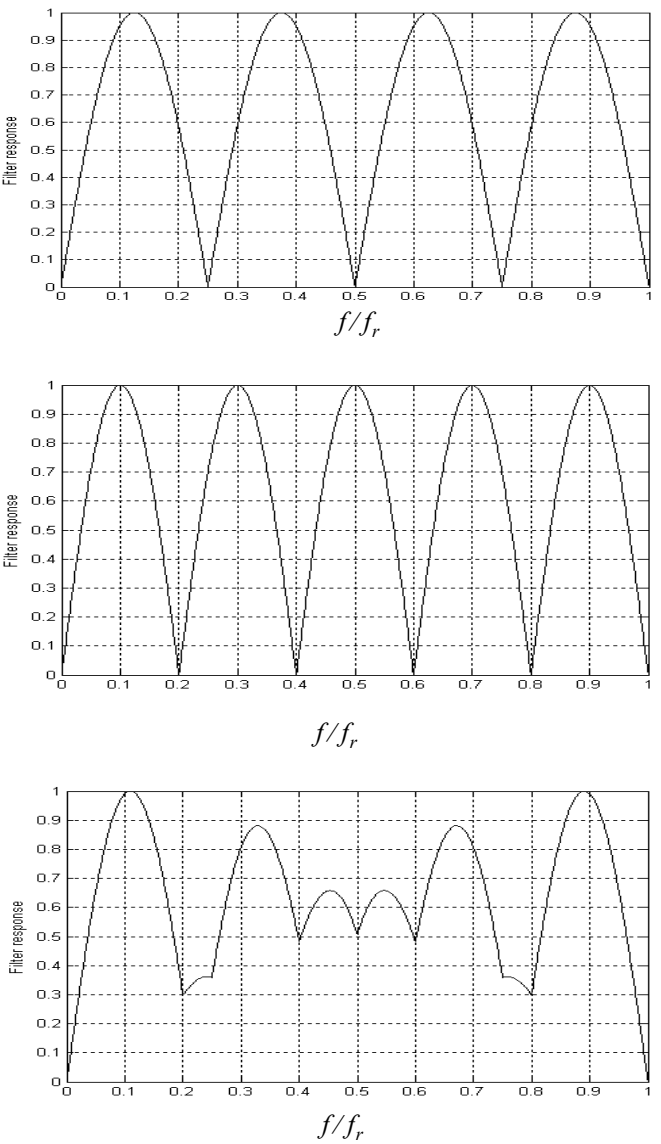

Figure 9.22. Frequency responses of a single canceler. Top plot corresponds to T_1, middle plot corresponds to T_2, bottom plot corresponds to stagger ratio $T_1/T_2 = 4/3$.

To better determine the frequency response of an MTI filter with staggered PRFs consider a three-pulse canceler with two PRFs, or equivalently two PRIs, T_1 and T_2. In this case, the impulse response will be given by

$$h(t) = [\delta(t) - \delta(t - T_1)] - [\delta(t - T_1) - \delta(t - T_1 - T_2)] \tag{9.87}$$

which can be written as

$$h(t) = \delta(t) - 2\delta(t - T_1) + \delta(t - T_1 - T_2) \tag{9.88}$$

Note that PRF staggering requires a minimum of two PRFs.

Make the change of variables $u = t - T_1$ in Eq. (9.88), and it follows

$$h(u + T_1) = \delta(u + T_1) - 2\delta(u) + \delta(u - T_2) \tag{9.89}$$

The Z-transform of the impulse response in Eq. (9.89) is then given by

$$H(z)z^{-T_1} = z^{T_1} - 2 + z^{-T_2} \tag{9.90}$$

and the amplitude frequency response for the staggered double delay line canceller is then given by

$$|H(z)|^2\Big|_{z = e^{j\omega T}} = (z^{T_1} - 2 + z^{-T_2})(z^{-T_1} - 2 + z^{T_2}) \tag{9.91}$$

Performing the algebraic manipulation in Eq. (9.91) and using the t trigonometric identity $(e^{j\omega T} + e^{-j\omega T}) = 2\cos\omega T$ yields

$$|H(\omega)|^2 = 6 - 4\cos(2\pi f T_1) - 4\cos(2\pi f T_2) + 2\cos(2\pi f(T_1 + T_2)) \tag{9.92}$$

It is customary to normalize the amplitude frequency response, thus

$$|H(\omega)|^2 = 1 - \frac{2}{3}\cos(2\pi f T_1) - \frac{2}{3}\cos(2\pi f T_2) + \frac{1}{3}\cos(2\pi f(T_1 + T_2)) \tag{9.93}$$

To determine the characteristics of higher stagger ratio MTI filters, adopt the notion of having several MTI filters, one for each combination of two staggered PRFs. Then the overall filter response is computed as the average of all individual filters. For example, consider the case where a PRF stagger is required with PRIs T_1, T_2, T_3, and T_4. First, compute the filter response using T_1 T_2 and denote by H_1. Then compute H_2 using T_2 and T_3, the filter H_3 is computed using T_3 T_4 and the filter H_4 is computed using T_4 and T_1. Finally compute the overall response as

$$H(f) = \frac{1}{4}[H_1(f) + H_2(f) + H_3(f) + H_4(f)] \tag{9.94}$$

Figure 9.23 shows the MTI filter response for a 4 stagger ratio defined. The overall response is computed as the average of 4 individual filters each corresponding to one combination of the stagger ratio. In the top portion of the figure the individual filters used were 2-pulse MTIs, while the bottom portion used 4-pulse individual MTI filters. This plot can be reproduced using the following MATLAB code.

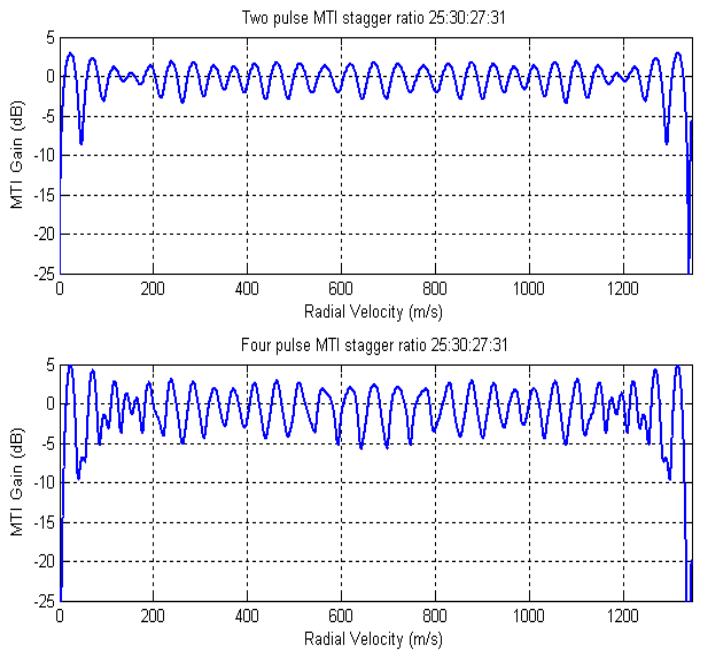

Figure 9.23. MTI responses with PRF staggering.

```
%Reproduce Fig 9.23 of text
k = .00035/25; a = 25*k; b = 30*k; c = 27*k; d = 31*k;
v2 = linspace(0,1345,10000);
f2 = (2.*v2)/.0375;
% H1(f)
T1 = exp(-j*2*pi.*f2*a); X1 = 1/2.*(1 - T1).*conj(1 - T1); H1 = 10*log10(abs(X1));
% H2(f)
T2 = exp(-j*2*pi.*f2*b); X2 = 1/2.*(1 - T2).*conj(1 - T2); H2 = 10*log10(abs(X2));
% H3(f)
T3 = exp(-j*2*pi.*f2*c); X3 = 1/2.*(1 - T3).*conj(1 - T3); H3 = 10*log10(abs(X3));
% H4(f)
T4 = exp(-j*2*pi.*f2*d); X4 = 1/2.*(1 - T4).*conj(1 - T4); H4 = 10*log10(abs(X4));
```

```
% Plot of the four components of H(f)
figure(1)
subplot(2,1,1)
% H(f) Average
ave2 = abs((X1 + X2 + X3 + X4)./4);
Have2 = 10*log10(abs((X1 + X2 + X3 + X4)./4));
plot(v2,Have2);
axis([0 1345 -25 5]);
 title('Two pulse MTI stagger ratio 25:30:27:31');
xlabel('Radial Velocity (m/s)');
 ylabel('MTI Gain (dB)'); grid on
% %Mean value of H(f)
v4 = v2; f4 = (2.*v4)/.0375;
% H1(f)
T1 = exp(-j*2*pi.*f4*a);
 T2 = exp(-j*2*pi.*f4*(a + b));
T3 = exp(-j*2*pi.*f4*(a + b + c));
X1 = 1/20.*(1 - 3.*T1 + 3.*T2 - T3).*conj(1 - 3.*T1 + 3.*T2 - T3);
H1 = 10*log10(abs(X1));
% H2(f)
T3 = exp(-j*2*pi.*f4*b);
T4 = exp(-j*2*pi.*f4*(b + c));
T5 = exp(-j*2*pi.*f4*(b + c + d));
X2 = 1/20.*(1 - 3.*T3 + 3.*T4 - T5).*conj(1 - 3.*T3 + 3.*T4 - T5);
H2 = 10*log10(abs(X2));
% H3(f)
T6 = exp(-j*2*pi.*f4*c);
T7 = exp(-j*2*pi.*f4*(c + d));
T8 = exp(-j*2*pi.*f4*(c + d + a));
X3 = 1/20.*(1 - 3.*T6 + 3.*T7 - T8).*conj(1 - 3.*T6 + 3.*T7 - T8);
H3 = 10*log10(abs(X3));
% H4(f)
T9 = exp(-j*2*pi.*f4*d); T10 = exp(-j*2*pi.*f4*(d + a));
T11 = exp(-j*2*pi.*f4*(d + a + b));
X4 = 1/20.*(1 - 3.*T9 + 3.*T10 - T11).*conj(1 - 3.*T9 + 3.*T10 - T11);
H4 = 10*log10(abs(X4));
% H(f) Average
ave4 = abs((X1 + X2 + X3 + X4)./4);
Have4 = 10*log10(abs((X1 + X2 + X3 + X4)./4));
% Plot of H(f) Average
subplot(2,1,2)
plot(v4,Have4);
axis([0 1345 -25 5]);
title('Four pulse MTI stagger ratio 25:30:27:31');
xlabel('Radial Velocity (m/s)');
ylabel('MTI Gain (dB)');
grid on
```

9.8. MTI Improvement Factor

In this section two quantities that are normally used to define the performance of MTI systems are introduced. They are Clutter Attenuation (CA) and the Improvement Factor. The MTI CA is defined as the ratio between the MTI filter input clutter power C_i to the output clutter power C_o,

$$CA = C_i / C_o \tag{9.95}$$

The MTI improvement factor is defined as the ratio of the SCR at the output to the SCR at the input,

$$I = \left(\frac{S_o}{C_o}\right) / \left(\frac{S_i}{C_i}\right) \tag{9.96}$$

which can be rewritten as

$$I = \frac{S_o}{S_i} CA \tag{9.97}$$

The ratio S_o / S_i is the average power gain of the MTI filter, and it is equal to $|H(\omega)|^2$. In this section, a closed form expression for the improvement factor using a Gaussian-shaped power spectrum (see Eq. (9.59)) is developed. A Gaussian-shaped clutter power spectrum is given by

$$S(f) = \frac{P_c}{\sqrt{2\pi}\ \sigma_f} \exp(-f^2 / 2\sigma_f^2) \tag{9.98}$$

where P_c is the clutter power (constant), and σ_f is the clutter rms frequency (which describes the clutter spectrum spread in the frequency domain, see Eq. (9.55)).

The clutter power at the input of an MTI filter is

$$C_i = \int_{-\infty}^{\infty} \frac{P_c}{\sqrt{2\pi}\ \sigma_f} \exp\left(-\frac{f^2}{2\sigma_f^2}\right) df \tag{9.99}$$

Factoring out the constant P_c yields

$$C_i = P_c \int_{-\infty}^{\infty} \frac{1}{\sqrt{2\pi}\sigma_f} \exp\left(-\frac{f^2}{2\sigma_f^2}\right) df \tag{9.100}$$

It follows that

$$C_i = P_c \tag{9.101}$$

The clutter power at the output of an MTI is

$$C_o = \int_{-\infty}^{\infty} S(f)|H(f)|^2 \, df \tag{9.102}$$

9.8.1. Two-Pulse MTI Case

In this section we will continue the analysis using a single delay line canceler. The frequency response for a single delay line canceler is

$$|H(f)|^2 = 4\left(\sin\left(\frac{\pi f}{f_r}\right)\right)^2 \tag{9.103}$$

It follows that

$$C_o = \int_{-\infty}^{\infty} \frac{P_c}{\sqrt{2\pi}\ \sigma_f} \exp\left(-\frac{f^2}{2\sigma_f^2}\right) 4\left(\sin\left(\frac{\pi f}{f_r}\right)\right)^2 \, df \tag{9.104}$$

Now, since clutter power will only be significant for small f, the ratio f/f_r is very small (i.e., $\sigma_f \ll f_r$). Consequently, by using the small angle approximation, Eq. (9.104) is approximated by

$$C_o \approx \int_{-\infty}^{\infty} \frac{P_c}{\sqrt{2\pi}\ \sigma_f} \exp\left(-\frac{f^2}{2\sigma_f^2}\right) 4\left(\frac{\pi f}{f_r}\right)^2 \, df \tag{9.105}$$

which can be rewritten as

$$C_o = \frac{4P_c\pi^2}{f_r^2} \int_{-\infty}^{\infty} \frac{1}{\sqrt{2\pi\sigma_f^2}} \exp\left(-\frac{f^2}{2\sigma_f^2}\right) f^2 \, df \tag{9.106}$$

The integral part in Eq. (9.106) is the second moment of a zero-mean Gaussian distribution with variance σ_f^2. Replacing the integral in Eq. (9.106) by σ_f^2 yields

$$C_o = \frac{4P_c\pi^2}{f_r^2}\ \sigma_f^2 \tag{9.107}$$

Substituting Eq. (9.107) and Eq. (9.101) into Eq. (9.95) produces

$$CA = \frac{C_i}{C_o} = \left(\frac{f_r}{2\pi\sigma_f}\right)^2 \tag{9.108}$$

It follows that the improvement factor for a single canceler is

$$I = \left(\frac{f_r}{2\pi\sigma_f}\right)^2 \frac{S_o}{S_i} \tag{9.109}$$

The power gain ratio for a single canceler is (remember that $|H(f)|$ is periodic with period f_r)

$$\frac{S_o}{S_i} = |H(f)|^2 = \frac{1}{f_r}\int_{-f_r/2}^{f_r/2} 4\left(\sin\frac{\pi f}{f_r}\right)^2 df \tag{9.110}$$

Using the trigonometric identity $(2 - 2\cos 2\vartheta) = 4(\sin\vartheta)^2$ yields

$$|H(f)|^2 = \frac{1}{f_r}\int_{-f_r/2}^{f_r/2}\left(2 - 2\cos\frac{2\pi f}{f_r}\right)df = 2 \tag{9.111}$$

It follows that

$$I = 2(f_r/2\pi\sigma_f)^2 \tag{9.112}$$

The expression given in Eq. (9.112) is an approximation valid only for $\sigma_f \ll f_r$. When the condition $\sigma_f \ll f_r$ is not true, then the autocorrelation function needs to be used in order to develop an exact expression for the improvement factor.

Example:

A certain radar has $f_r = 800Hz$. If the clutter rms is $\sigma_f = 6.4Hz$, find the improvement factor when a single delay line canceler is used.

Solution:

The clutter attenuation CA is

$$CA = \left(\frac{f_r}{2\pi\sigma_f}\right)^2 = \left(\frac{800}{(2\pi)(6.4)}\right)^2 = 395.771 = 25.974dB$$

and since $S_o/S_i = 2 = 3dB$ we get

$$I_{dB} = (CA + S_o/S_i)_{dB} = 3 + 25.97 = 28.974dB.$$

9.8.2. The General Case

A general expression for the improvement factor for the n-pulse MTI (shown for a 2-pulse MTI in Eq. (9.112)) is given by

$$I = \frac{1}{Q^2(2(n-1)-1)!!}\left(\frac{f_r}{2\pi\sigma_f}\right)^{2(n-1)} \tag{9.113}$$

where the double factorial notation is defined by

$$(2n-1)!! = 1 \times 3 \times 5 \times \ldots \times (2n-1) \tag{9.114}$$

$$(2n)!! = 2 \times 4 \times \ldots \times 2n \tag{9.115}$$

Of course $0!! = 1$; Q is defined by

$$Q^2 = \frac{1}{n} \tag{9.116}$$
$$\sum A_i^2$$

where A_i are the binomial coefficients for the MTI filter. It follows that Q^2 for a 2-pulse, 3-pulse, and 4-pulse MTI are, respectively,

$$\left\{\frac{1}{2}, \frac{1}{20}, \frac{1}{70}\right\} \tag{9.117}$$

Using this notation, then the improvement factor for a 3-pulse and 4-pulse MTI are, respectively, given by

$$I_{3-pulse} = 2\left(\frac{f_r}{2\pi\sigma_t}\right)^4 \tag{9.118}$$

$$I_{4-pulse} = \frac{4}{3}\left(\frac{f_r}{2\pi\sigma_t}\right)^6 \tag{9.119}$$

9.9. Subclutter Visibility (SCV)

Subclutter Visibility (SCV) describes the radar's ability to detect nonstationary targets embedded in a strong clutter background, for some probabilities of detection and false alarm. It is often used as a measure of MTI performance. For example, a radar with $10dB$ SCV will be able to detect moving targets whose returns are ten times smaller than those of clutter. A sketch illustrating the concept of SCV is shown in Fig. 9.24.

If a radar system can resolve the areas of strong and weak clutter within its field of view, then Interclutter Visibility (ICV) describes the radar's ability to detect nonstationary targets between strong clutter points. The subclutter visibility is expressed as the ratio of the improvement factor to the minimum MTI

output SCR required for proper detection for a given probability of detection. More precisely,

$$SCV = I/(SCR)_o \tag{9.120}$$

When comparing the performance of different radar systems on the basis of SCV, one should use caution since the amount of clutter power is dependent on the radar resolution cell (or volume), which may be different from one radar to another. Thus, only if the different radars have the same beamwidths and the same pulse widths can SCV be used as a basis of performance comparison.

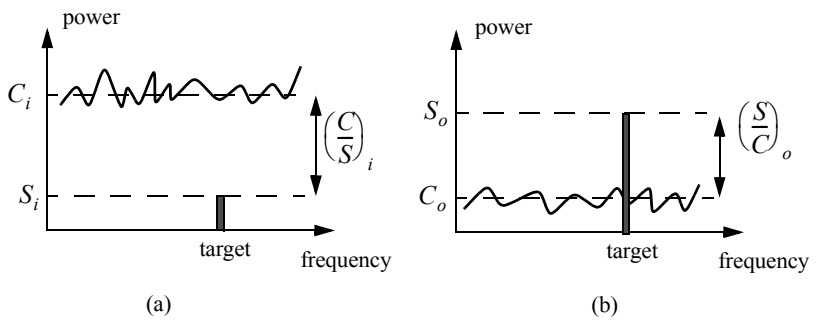

Figure 9.24. Illustration of SCV. (a) MTI input. (b) MTI output.

9.10. Delay Line Cancelers with Optimal Weights

The delay line cancelers discussed in this chapter belong to a family of transversal Finite Impulse Response (FIR) filters widely known as the "tapped delay line" filters. Figure 9.25 shows an N-stage tapped delay line implementation. When the weights are chosen such that they are the binomial coefficients (coefficients of the expansion $(1-x)^N$) with alternating signs, then the resultant MTI filter is equivalent to N-stage cascaded single line cancelers. This is illustrated in Fig. 9.26 for $N = 4$. In general, the binomial coefficients are given by

$$w_i = (-1)^{i-1} \frac{N!}{(N-i+1)!(i-1)!} \; ; \; i = 1, \ldots, N+1 \tag{9.121}$$

Using the binomial coefficients with alternating signs produces an MTI filter that closely approximates the optimal filter in the sense that it maximizes the improvement factor, as well as the probability of detection. In fact, the difference between an optimal filter and one with binomial coefficients is so small that the latter one is considered to be optimal by most radar designers. How-

ever, being optimal in the sense of the improvement factor does not guarantee a deep notch or a flat pass-band in the MTI filter response. Consequently, many researchers have been investigating other weights that can produce a deeper notch around DC, as well as a better pass-band response.

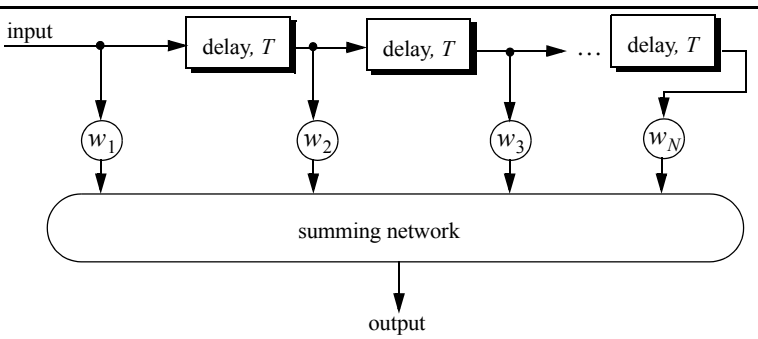

Figure 9.25. N-stage tapped delay line filter.

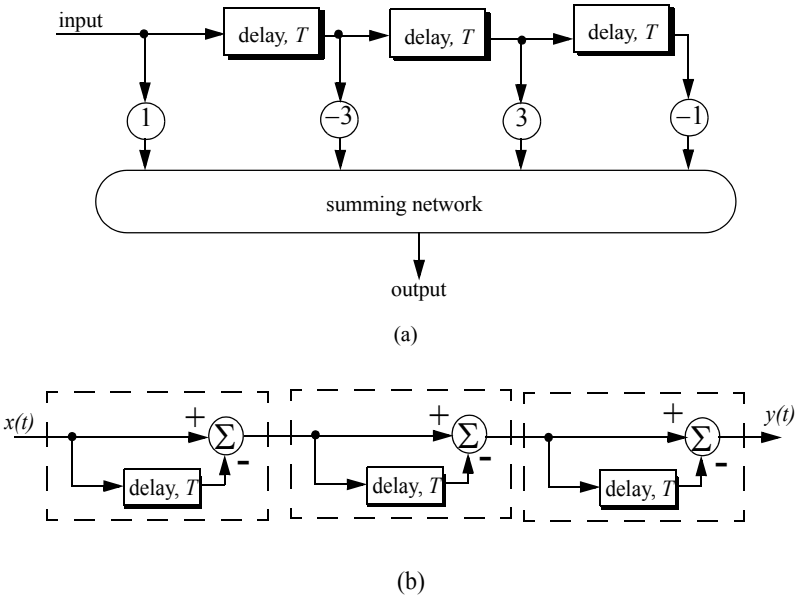

Figure 9.26. Two equivalent three delay line cancelers. (a) Tapped delay line. (b) Three cascaded single line cancelers.

In general, the average power gain for an N-stage delay line canceler is

$$\frac{S_o}{S_i} = \prod_{i=1}^{N} |H_1(f)|^2 = \prod_{i=1}^{N} 4\left(\sin\left(\frac{\pi f}{f_r}\right)\right)^2 \tag{9.122}$$

For example, $N = 2$ (double delay line canceler) gives

$$\frac{S_o}{S_i} = 16\left(\sin\left(\frac{\pi f}{f_r}\right)\right)^4 \tag{9.123}$$

Equation (9.123) can be rewritten as

$$\frac{S_o}{S_i} = |H_1(f)|^{2N} = 2^{2N}\left(\sin\left(\frac{\pi f}{f_r}\right)\right)^{2N} \tag{9.124}$$

As indicated by Eq. (9.124), blind speeds for an N-stage delay canceler are identical to those of a single canceler. It follows that blind speeds are independent from the number of cancelers used. It is possible to show that Eq. (9.124) can be written as

$$\frac{S_o}{S_i} = 1 + N^2 + \left(\frac{N(N-1)}{2!}\right)^2 + \left(\frac{N(N-1)(N-2)}{3!}\right)^2 + \ldots \tag{9.125}$$

A general expression for the improvement factor of an N-stage tapped delay line canceler is reported by Nathanson[1] to be

$$I = \frac{(S_o/S_i)}{\sum_{k=1}^{N}\sum_{j=1}^{N} w_k w_j^* \rho\left(\frac{(k-j)}{f_r}\right)} \tag{9.126}$$

where the weights w_k and w_j are those of a tapped delay line canceler, and $\rho((k-j)/f_r)$ is the correlation coefficient between the kth and jth samples. For example, $N = 2$ produces

$$I = \frac{1}{1 - \frac{4}{3}\rho T + \frac{1}{3}\rho 2T} \tag{9.127}$$

1. Nathanson, F. E., *Radar Design Principles*, 2nd edition, McGraw-Hill, Inc., NY, 1991.

9.11. MATLAB Program Listings

This section presents listings for all the MATLAB programs used to produce all of the MATLAB-generated figures in this chapter. They are listed in the same order they appear in the text.

9.11.1. MATLAB Function "clutter_rcs.m"

The function *"clutter_rcs.m"* implements Eq. (9.37). It generates plots of the clutter RCS versus the radar slant range. Its outputs include the clutter RCS in dBsm. The syntax is as follows:

function [sigmaC] = clutter_rcs(sigma0, thetaE, thetaA, SL, range, hr, ht, b,ant_id)

where

Symbol	Description	Units	Status
sigma0	*clutter back scatterer coefficient*	*dB*	*input*
thetaE	*antenna 3dB elevation beamwidth*	*degrees*	*input*
thetaA	*antenna 3dB azimuth beamwidth*	*degrees*	*input*
SL	*antenna sidelobe level*	*dB*	*input*
range	*range; can be a vector or a single value*	*Km*	*input*
hr	*radar height*	*meters*	*input*
ht	*target height*	*meters*	*input*
b	*bandwidth*	*Hz*	*input*
ant_id	*1 for (sin(x)/x)^2 pattern* *2 for Gaussian pattern*	*none*	*input*
sigmac	*clutter RCS; can be either vector or single value depending on "range"*	*dB*	*output*

A GUI called *"clutter_rcs_gui"* was developed for this function. Executing this GUI generates plots of the σ_c versus range. Figure 9.26 shows the GUI workspace associated with this function.

MATLAB Function "clutter_rcs.m" Listing

```
function [sigmaC] = clutter_rcs(sigma0, thetaE, thetaA, SL, range, hr, ht, b,ant_id)
% This unction calculates the clutter RCS and the CNR for a ground based radar.
thetaA = thetaA * pi /180; % antenna azimuth beamwidth in radians
thetaE = thetaE * pi /180.; % antenna elevation beamwidth in radians
re = 6371000; % earth radius in meter
rh = sqrt(8.0*hr*re/3.); % range to horizon in meters
```

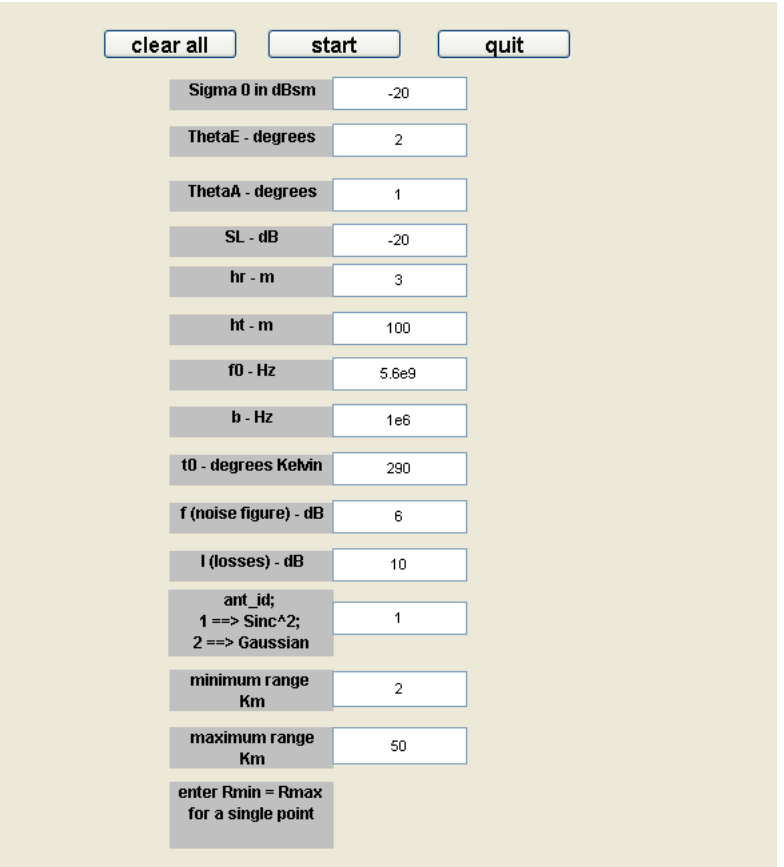

Figure 9.27. GUI workspace for *"clutter_rcs_gui.m."*

```
SLv = 10.0^(SL/10); % radar rms sidelobes in volts
sigma0v = 10.0^(sigma0/10); % clutter backscatter coefficient
deltar = 3e8 / 2 / b; % range resolution for unmodulated pulse
range_m = 1000 .* range;  % range in meters
%%%%%%%%%%%%%%%%%%%%%%%%%%%%%%%%%%%%
thetar = asin(hr ./ range_m);
thetae = asin((ht-hr) ./ range_m);
% propagation attenuation due to round earth
propag_atten = 1. + ((range_m ./ rh).^4);
Rg = range_m .* cos(thetar);
deltaRg = deltar .* cos(thetar);
theta_sum = thetae + thetar;
% use sinc^2 antenna pattern when ant_id=1
```

```
% use Gaussian antenna pattern when ant_id=2
if(ant_id ==1) % use sinc^2 antenna pattern
   ant_arg = (theta_sum ) ./ (pi*thetaE);
   gain = (sinc(ant_arg)).^2;
else
   gain = exp(-2.776 .*(theta_sum./thetaE).^2);
end
% compute sigmac
sigmac = (sigma0v . * Rg . * deltaRg) . * ...
(pi * SLv * SLv + thetaA . * gain.^2) ./ propag_atten;
sigmaC = 10*log10(sigmac);
figure(1)
plot(range, sigmaC,'linewidth',1.5)
grid
xlabel('Slant Range in Km')
ylabel('Clutter RCS in dBsm')
%
```

9.11.2. MATLAB Function "single_canceler.m"

The function *"single_canceler.m"* computes and plots (as a function of f/f_r) the amplitude response for a single delay line canceler. The syntax is as follows:

$$[resp] = single\_canceler\ (fofr)$$

where *"fofr"* is the number of periods desired.

MATLAB Function** "single_canceler.m" **Listing

```
function [resp] = single_canceler (fofr1)
% single delay canceller
eps = 0.00001;
fofr = 0:0.01:fofr1;
arg1 = pi .* fofr;
resp = 4.0 .*((sin(arg1)).^2);
max1 = max(resp);
resp = resp ./ max1;
subplot(2,1,1)
plot(fofr,resp,'k')
xlabel ('Normalized frequency in f/fr')
ylabel( 'Amplitude response in Volts')
grid
subplot(2,1,2)
resp=10.*log10(resp+eps);
plot(fofr,resp,'k');
axis tight
grid
xlabel ('Normalized frequency in f/fr')
```

```
ylabel( 'Amplitude response in dB')
```

9.11.3. MATLAB Function "double_canceler.m"

The function *"double_canceler.m"* computes and plots (as a function of f/f_r) the amplitude response for a double delay line canceler. The syntax is as follows:

$$[resp] = double\_canceler\ (fofr)$$

where *"fofr"* is the number of periods desired.

MATLAB Function** "double_canceler.m" **Listing

```
function [resp] = double_canceler(fofr1)
eps = 0.00001;
fofr = 0:0.01:fofr1;
arg1 = pi .* fofr;
resp = 4.0 .* ((sin(arg1)).^2);
max1 = max(resp);
resp = resp ./ max1;
resp2 = resp .* resp;
subplot(2,1,1);
plot(fofr,resp,'k--',fofr, resp2,'k');
ylabel ('Amplitude response - Volts')
resp2 = 20. .* log10(resp2+eps);
resp1 = 20. .* log10(resp+eps);
subplot(2,1,2)
plot(fofr,resp1,'k--',fofr,resp2,'k');
legend ('single canceler','double canceler')
xlabel ('Normalized frequency f/fr')
ylabel ('Amplitude response in dB')
```

Problems

9.1. Compute the signal-to-clutter ratio (SCR) for the radar described in Section 9.2.1. In this case, assume antenna 3dB beam width $\theta_{3dB} = 0.03rad$, pulse width $\tau = 10\mu s$, range $R = 50Km$, grazing angle $\psi_g = 15°$, target RCS $\sigma_t = 0.1m^2$, and clutter reflection coefficient $\sigma^0 = 0.02(m^2/m^2)$.

9.2. Repeat the example in Section 9.3 for target RCS $\sigma_t = 0.15m^2$, pulse width $\tau = 0.1\mu s$, antenna beam width $\theta_a = \theta_e = 0.03radians$; the detection range is $R = 100Km$, and $\sum \sigma_i = 1.6 \times 10^{-9}(m^2/m^3)$.

9.3. The quadrature components of the clutter power spectrum are, respectively, given by

$$\bar{S}_I(f) = \delta(f) + \frac{C}{\sqrt{2\pi}\sigma_c}\exp(-f^2/2\sigma_c^2)$$

and

$$\overline{S_Q}(f) = \frac{C}{\sqrt{2\pi}\sigma_c}\exp(-f^2/2\sigma_c^2).$$

Compute the D.C. and A.C. power of the clutter. Let $\sigma_c = 10Hz$.

9.4. A certain radar has the following specifications: pulse width $\tau' = 1\mu s$, antenna beam width $\Omega = 1.5°$, and wavelength $\lambda = 3cm$. The radar antenna is $7.5m$ high. A certain target is simulated by two point targets (scatterers). The first scatterer is $4m$ high and has RCS $\sigma_1 = 20m^2$. The second scatterer is $12m$ high and has RCS $\sigma_2 = 1m^2$. If the target is detected at $10Km$, compute (a) SCR when both scatterers are observed by the radar, (b) SCR when only the first scatterer is observed by the radar. Assume a reflection coefficient of -1, and $\sigma^0 = -30dB$.

9.5. A certain radar has range resolution of $300m$ and is observing a target somewhere in a line of high towers each having RCS $\sigma_{tower} = 10^6 m^2$. If the target has RCS $\sigma_t = 1m^2$, (a) how much signal-to-clutter ratio should the radar have? (b) Repeat part (a) for range resolution of $30m$.

9.6. (a) Derive an expression for the impulse response of a single delay line canceler. (b) Repeat for a double delay line canceler.

9.7. (a) What is the transfer function, $H(z)$? (b) If the clutter power spectrum is $W(f) = w_0\exp(-f^2/2\sigma_c^2)$, find an exact expression for the filter power gain. (c) Repeat part (b) for small values of frequency, f. (d) Compute the clutter attenuation and the improvement factor in terms of K and σ_c.

9.8. One implementation of a single delay line canceler with feedback is shown below

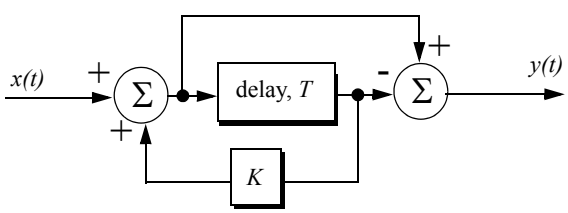

9.9. Plot the frequency response for the filter described in the previous problem for $K = -0.5, 0, and\ 0.5$.

9.10. An implementation of a double delay line canceler with feedback is shown below.

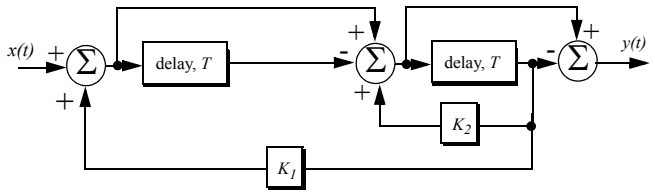

(a) What is the transfer function, $H(z)$? (b) Plot the frequency response for $K_1 = 0 = K_2$, and $K_1 = 0.2, K_2 = 0.5$.

9.11. Consider a single delay line canceler. Calculate the clutter attenuation and the improvement factor. Assume that $\sigma_c = 4Hz$ and PRF $f_r = 450Hz$.

9.12. Develop an expression for the improvement factor of a double delay line canceler.

9.13. Repeat Problem 9.10 for a double delay line canceler.

9.14. An experimental expression for the clutter power spectrum density is $W(f) = w_0 \exp(-f^2/2\sigma_c^2)$, where w_0 is a constant. Show that using this expression leads to the same result obtained for the improvement factor as developed in Section 9.8.

9.15. A certain radar uses two PRFs with stagger ratio 63/64. If the first PRF is $f_{r1} = 500Hz$, compute the blind speeds for both PRFs and for the resultant composite PRF. Assume $\lambda = 3cm$.

9.16. A certain filter used for clutter rejection has an impulse response $h(n) = \delta(n) - 3\delta(n-1) + 3\delta(n-2) - \delta(n-3)$. (a) Show an implementation of this filter using delay lines and adders. (b) What is the transfer function? (c) Plot the frequency response of this filter. (d) Calculate the output when the input is the unit step sequence.

9.17. The quadrature components of the clutter power spectrum are given in Problem 9.3. Let $\sigma_c = 10Hz$ and $f_r = 500Hz$. Compute the improvement of the signal-to-clutter ratio when a double delay line canceler is utilized.

9.18. Develop an expression for the clutter improvement factor for single and double line cancelers using the clutter autocorrelation function.